INL/RPT-23-75037
Revision 0

High-Fluence Active Irradiation and Combined Effects Testing of Sapphire Optical Fiber Distributed Temperature Sensors

September 2023

Final Report

Kelly M. McCary
Idaho National Laboratory, Chemical and Radiation Measurement Department

Joshua Daw
Idaho National Laboratory, Measurement Science Department

Thomas E. Blue
The Ohio State University, Nuclear Engineering Program, Mechanical & Aerospace Engineering Department

Idaho National Laboratory

INL is a U.S. Department of Energy National Laboratory operated by Battelle Energy Alliance, LLC

DISCLAIMER

This information was prepared as an account of work sponsored by an agency of the U.S. Government. Neither the U.S. Government nor any agency thereof, nor any of their employees, makes any warranty, expressed or implied, or assumes any legal liability or responsibility for the accuracy, completeness, or usefulness, of any information, apparatus, product, or process disclosed, or represents that its use would not infringe privately owned rights. References herein to any specific commercial product, process, or service by trade name, trademark, manufacturer, or otherwise, does not necessarily constitute or imply its endorsement, recommendation, or favoring by the U.S. Government or any agency thereof. The views and opinions of authors expressed herein do not necessarily state or reflect those of the U.S. Government or any agency thereof.

INL/RPT-23-75037
Revision 0

High-Fluence Active Irradiation and Combined Effects Testing of Sapphire Optical Fiber Distributed Temperature Sensors

Final Report

Kelly M. McCary
Idaho National Laboratory, Chemical and Radiation Measurement Department
Joshua Daw
Idaho National Laboratory, Measurement Science Department
Thomas E. Blue
The Ohio State University, Nuclear Engineering Program, Mechanical & Aerospace

September 2023

Idaho National Laboratory
Measurement Science Department/Radiation Measurements Laboratory
Idaho Falls, Idaho 83415

Prepared for the
U.S. Department of Energy
Office of Nuclear Energy
Under DOE Idaho Operations Office
Contract DE-AC07-05ID14517

Page intentionally left blank

ABSTRACT

The goal of this work was to investigate the in-core performance of sapphire optical fiber temperature sensors and to develop clad sapphire optical fibers for in-core instrumentation. We fabricated clad sapphire optical fibers and evaluated the distributed sensing performance of these sensors via optical backscatter reflectometry under high fluence and combined radiation and temperature effects. A series of irradiations was completed to evaluate the effect of irradiation on sapphire optical fiber temperature sensors and to determine the operational limits of these sensors.

- Objective 1: Fabricate sapphire optical fiber sensors.
- Objective 2: Evaluate the clad sapphire fiber to verify single-mode behavior and determine and characterize the light modes supported by optical fibers.
- Objective 3: Characterize the in-core temperature sensing of sapphire optical fiber, as well as the combined temperature and irradiation effects.
- Objective 4: Evaluate the lifetime and performance of the sensor under irradiation to high neutron fluence.

Objectives 1, 2, and 3 were completed during the first 2 years of the project. Due to the Covid pandemic, Objective 4, a high-fluence irradiation performed at the Massachusetts Institute of Technology Research Reactor (MITR), was delayed, as partner facilities were subject to mandatory shutdowns and required a 1 year, no-cost extension. This irradiation was eventually completed on December 12, 2022. This work indicates that sapphire optical fiber sensors may be a solution for ultra-high-temperature applications in which traditional silica optical fibers are prone to fail. Sapphire sensors are potentially suitable for experiments featuring temperatures above 700°C for long periods of time, or for any length of time above 1000°C. Experiments featuring a low total fluence, such as irradiations conducted in the Transient Reactor Test (TREAT) facility, also represent good applications for sapphire optical sensors. Additional work is required to characterize the sapphire fiber cladding performance, which falls outside the scope of this project, as well as the effects of high temperatures on the response of the fiber. A comprehensive material study is recommended as future work to evaluate the attenuation in sapphire under irradiation, and how that attenuation changes with irradiation temperature. The drift and attenuation in the fiber at temperatures of up to 1600°C and a total fluence of up to 2.9×10^{17} n/cm^2 was minimal, and the fibers returned to baseline after being heated to 1600°C under irradiation. This is promising for the future use of sapphire optical fibers in advanced reactors.

Page intentionally left blank

ACKNOWLEDGMENTS

The authors wish to acknowledge and thank the staff at the Ohio State University Research Reactor and the Massachusetts Institute of Technology Reactor—Dr. Susan White, Andrew Kauffman, Matthew Van Zile, Joel Hatch, and David Carpenter—for their flexibility, technical advice, and support. Special thanks to Josh Jones, a graduate student at The Ohio State University, for his time and assistance in fiber preparation for the cladding irradiations, as well as for his involvement in the fiber extractions and for providing valuable input on fiber postprocessing. Thanks also to Anthony Birri, a former graduate student at The Ohio State University and now a researcher at Oak Ridge National Laboratory, for his assistance with fiber extraction and the heated irradiation.

Page intentionally left blank

CONTENTS

FIGURES

TABLES

Page intentionally left blank

ACRONYMS

FBG	fiber Bragg grating
ISCA	In-core Sample Assembly
MIT	Massachusetts Institute of Technology
MITR	Massachusetts Institute of Technology Research Reactor
NRL	Nuclear Reactor Laboratory
OBR	Optical Backscatter Reflectometer
OD	Outer Diameter
OFDR	Optical Frequency Domain Reflectometry
OSU	The Ohio State University
OSURR	Ohio State University Research Reactor
TREAT	Transient Reactor Test Facility

Page intentionally left blank

High-Fluence Active Irradiation and Combined Effects Testing of Sapphire Optical Fiber Distributed Temperature Sensors

1. INTRODUCTION

This report summarizes the testing and characterization of distributed temperature measurements when using sapphire optical fiber for high-temperature radiation environments. Separate effects testing of high fluence and combined effects testing of heated irradiations were performed to characterize the sensing capability of clad sapphire optical fiber. Creation of innovative measurement techniques will support testing and development of advanced fuels and materials for the current U.S. reactor fleet, as well as the design of advanced reactors.

Section 2 of this report provides background information on the overall aim of the project, the research to be conducted, and the benefits of this research. Section 3 covers the current and planned status of the remaining project objectives and deliverables. Section 4 discusses the results of work conducted over the previous year, and Section 5 presents the results of the long-duration irradiation performed at the Massachusetts Institute of Technology (MIT) Nuclear Reactor Laboratory (NRL). Section 6 summarizes the report and offers recommendations for future development work.

2. BACKGROUND

Advanced fuels and materials are being developed to improve the performance of the current U.S. nuclear fleet and to support the design of advanced reactors. These new fuel designs require a better understanding of radiation effects. Currently, researchers rely on irradiation experiments that cover a wide range of behaviors: from separate effects to more integral (combined) effects that underpin prototypic conditions. Innovative measurement techniques for collecting real-time data during experiments are needed to overcome the limitations of empirical approaches based on post-irradiation examination. For the present project, researchers employed optical backscatter reflectometry methods to test the effects, both separate and combined, of high fluence and high temperature on the temperature-sensing capabilities of clad sapphire optical fiber. Current fiber optic sensors based on standard fused silica have demonstrated the capability to provide multi-modal sensing (i.e., measuring values such as temperature, pressure, and strain with a single sensor configuration) and multiplexing (communicating data collected at multiple locations through a single line). They are intrinsically immune to electromagnetic interference, are electrically passive, are compatible with a number of different sensing methodologies, and are widely available at reasonable cost. Widely known for their use in the telecommunications field, instruments based on silica fibers have already been deployed in industrial applications—at temperatures approaching 300–400°C—for enabling distributed temperature sensing in oil and gas recovery activities. At temperatures above 500°C, conventional silica fibers may suffer from instabilities caused by interactions with various environmental species, especially hydrogen and/or water. While protective coatings can alleviate some such environmental concerns, the amorphous structure of fused silica indicates inherent instability when approaching the so-called "annealing" temperature (1,000–1,100°C) at which the silica networks recrystallize. Fused silica is also strongly impacted by radiation. At the macroscopic scale, three mechanisms are responsible for degraded performance of the fiber: radiation-induced attenuation, which increases light adsorption in the material (darkening); radiation-induced emission, which generates unwanted light (optical noise); and radiation-induced compaction, which causes variations in the density of the fiber material, thus altering its optical properties.

Sapphire (α-Al_2O_3) fibers are recognized as a high-temperature alternative to amorphous silica, thanks to their high melting temperature (about 2,054°C) and outstanding chemical resistance, as well as the mechanical strength of their crystalline network. Their wide transmission window and high damage threshold make them an ideal candidate for multiple sensing techniques used for measuring temperature, strain, deformation, pressure, and chemical composition in extreme environments. The outcome of this research will be to deliver modern optical fiber sensing techniques usable in various extreme environment applications. In the field of nuclear fuel/materials testing, these fibers will, during irradiation testing, provide access to operational data with excellent time and space resolution. Accurate online monitoring of test parameters such as temperature and strain will foster great reductions in the time and cost associated with developing, demonstrating, and licensing new nuclear technologies.

3. TASK STATUS

Successful completion of this work requires several different stages of the project. Three stages of irradiations were completed. The first includes cladding the sapphire optical fibers in a series of irradiations at the OSURR. The second is a heated irradiation of the sensors at the OSURR. The third stage is a high fluence irradiation of sensors at MITR.

3.1 Cladding Irradiations

As of March 19, 2021, all four cladding irradiations have been completed at The Ohio State University Research Reactor (OSURR), with a total of 14 clad optical fibers having been fabricated. Table 1 shows the current fiber inventory for this project. All 14 of the clad fibers have also been extracted. Of these, five were deployed in the heated irradiation conducted at The Ohio State University (OSU). All the fibers were purchased from MicroMaterials Inc.

Table 1. Current sapphire fiber inventory.

Quantity	# of FBGs	Inscribed by	OD (um)	Length	Location	Annealing	Notes
1	2	U-Pitt	100	13 in.	OSURR	1500℃ in air	Used in the heated OSURR irradiation
1	1 (was 2)	U-Pitt	100	16.25 in.	OSURR	1500℃ in air	Used in the heated OSURR irradiation—1 grating was lost due to breakage during handling
1	1	U-Pitt	100	15.25 in.	OSURR	1200℃ in air	Used in the heated OSURR irradiation
1	1	U-Pitt	100	~14 in.	OSU-Blue Lab	N/A	Extracted, at Blue Lab
1	1	U-Pitt	100	~14 in.	OSU-Blue Lab	N/A	Extracted, at Blue Lab
1	1	U-Pitt	100	~14 in.	OSU-Blue Lab	N/A	Extracted, at Blue Lab
1/2	0	N/A	100	9.25 in.	OSURR	1500℃ in air	Used in the heated OSURR irradiation—one half of a fiber that was split
1/2	0	N/A	100	8 in.	OSU-Blue Lab	N/A	Extracted, at Blue Lab—one half of a fiber that was split
1	13	FemtoFiberTec	75	23.5 in.	OSURR	1500℃ in air	Used in the heated OSURR irradiation
6	4	FemtoFiberTec	125	24 in.	OSU-Blue Lab	N/A	Extracted, at Blue Lab

3.2 Heated Irradiation

The heated irradiation at OSURR became ready for insertion on March 23, 2021. The irradiation ran from March 26 to April 21, 2021. In total, seven sensors were prepared for the heated irradiation: five sapphire optical fiber sensors and two silica optical fiber sensors. Unforeseen issues with the test vessel furnace arose during the irradiation, causing a delay to fix the furnace in the middle of the originally scheduled irradiation; however, all the days of the irradiation were completed, and temperatures of up to 1600°C were achieved in-core.

3.3 Long-Duration Irradiation

The long-duration irradiation at the MIT research reactor (MITR) is now complete. Table 2 shows the planned and actual completion dates for the different stages of this irradiation. The completion dates were delayed from what was initially planned, due to the Covid-19 pandemic and the fiber procurement and inscription delays discussed in PRS/EXT-20-00672, "Year 1 Status Report for Sapphire Irradiation Experiments." [1]

Table 2. Planned and actual completion dates for the long-duration irradiation conducted at MITR.

Deliverable Item	**Due Date**	**Assigned to**	**Completed**
Preliminary Sample and Test Matrix Established	10/30/2020	PI	10/30/2020
Sample and Test Matrix Finalized	12/18/2020	PI	02/18/2022
Test/Evaluation Sample(s) Delivered to NRL	10/29/2021	PI	3/14/2022
Sample Delivered to NRL	11/5/2021	PI	04/01/2022
Facility/Capsule Fabrication Completed	12/3/2021	NRL	04/20/2022
Facility/Capsule Made Ready for Insertion (Department of Energy Milestone)	12/31/2021	NRL	7/8/2022
Projected Irradiation Start Date (2 cycles)	1/21/2022	NRL	7/19/2022
Projected Irradiation Completion	7/1/2022	NRL	12/12/2022
Facility Irradiation Data Report Delivered to PI	8/1/2022	NRL	8/28/2023

4. SUMMARY OF PRIOR YEAR RESULTS

4.1 Fiber Fabrication and Preparation

Single-crystal sapphire fibers require several pretreatments before they are suitable for use with optical frequency domain reflectometry (OFDR) sensing. These include performing fiber Bragg grating (FBG) inscription, creating an internal cladding, heat treating the fiber after the cladding process, and applying mode stripping techniques. The fibers used in this project were all procured from MicroMaterials Inc. [2], then inscribed with FBGs from various sources.

4.1.1 Fiber Cladding

The fiber clad process involves packing sapphire optical fibers into aluminum tubes filled with Li-6 enriched lithium carbonate powder. The tubes are sealed, placed inside a second containment tube, and irradiated in OSURR to create a damage layer on the outer diameter (OD) of the sapphire fiber in order to generate a near-single-mode waveguide. [3] After irradiation, the fibers are taken from the tubes and cleaned to remove any remaining lithium carbonate powder. Four clad irradiations were completed over the course of this work, and descriptions of the fibers used in each cladding irradiation are listed below. Clad irradiations #1 and #2 were completed in fiscal year 2020, and irradiations #3 and #4 were completed in fiscal year 2021.

Clad Irradiation #1:

- Status: **Completed January 24, 2019**
- Fibers:
    - 100 um OD, 2 FBGs inscribed by U. Pitt, 13 in. long
    - 100 um OD, 2 FBGs inscribed by U. Pitt, 16.25 in. long
    - 100 um OD, no FBGs, 18 in. long
    - 75 um OD, 13 FBGs inscribed by FemtoFiberTec, 23.4 in. long

Clad Irradiation #2:

- Status: **Completed March 13, 2020**
- Fibers:
    - 100 um OD, 1 FBG inscribed by U. Pitt, ~15 in. long
    - 100 um OD, 1 FBG inscribed by U. Pitt, ~15 in. long
    - 100 um OD, 1 FBG inscribed by U. Pitt, ~15 in. long
    - 100 um OD, 1 FBG inscribed by U. Pitt, ~15 in. long

Clad Irradiation #3:

- Status: **Completed March 12, 2021**
- Fibers:
    - 125 um OD, 4 FBGs inscribed by FemtoFiberTec, 24 in. long
    - 125 um OD, 4 FBGs inscribed by FemtoFiberTec, 24 in. long
    - 75 um OD, 6 FBGs inscribed by FemtoFiberTec, 14 in. long

Clad Irradiation #4:

- Status: **Completed March 19, 2021**
- Fibers:
    - 125 um OD, 4 FBGs inscribed by FemtoFiberTec, 24 in. long
    - 125 um OD, 4 FBGs inscribed by FemtoFiberTec, 24 in. long
    - 125 um OD, 4 FBGs inscribed by FemtoFiberTec, 24 in. long
    - 125 um OD, 4 FBGs inscribed by FemtoFiberTec, 24 in. long.

4.1.2 Fiber Postprocessing

The clad sapphire fibers require annealing and additional postprocessing prior to use as OFDR sensors. The postprocessing includes a thermal annealing, a mode stripping treatment, polishing, and splicing. Table 1 lists the temperatures that some of the fibers were annealed to. These temperatures were chosen based on previous investigations of hydrogen implementation in sapphire. [4] To splice the sapphire fiber to a silica lead-out fiber so as to enable interrogation using the Luna optical backscatter reflectometer (OBR) 4600, the sapphire fiber must first be polished to a flat 90-degree face. Splicing the sapphire fiber to the silica fiber is made difficult by the vastly different melting temperatures of silica and sapphire. This work essentially used a cold splice in which the silica fiber was tapered down and around the sapphire fiber. This type of connection is inconsistent and often requires multiple attempts to properly establish. [5]

4.2 Fiber Characterization: Out-of-Core Testing

The sapphire optical fiber sensors were tested in a box furnace at up to 1500℃ prior to being deployed in OSURR. The box furnace, shown in Figure 1, has an 8-in. heated region, and the fibers were interrogated using the Luna OBR 4600. All the fibers were placed into alumina tubes that were closed on the heated ends and spliced to silica lead-out fibers. Figure 2 shows a plot of the responses of three of the FBGs in the 75-um-OD sapphire optical fiber with gratings inscribed by FemtoFiberTec. [6] These three FBGs were chosen because they were well within the heated region of the box furnace. The fiber responds well at 1100℃ and under. When the furnace is heated past 1100℃, the sensing mechanism fails—not due to a failure in the fiber, but to the wavelength range of the interrogator.

Figure 1. Box furnace used for out-of-core testing.

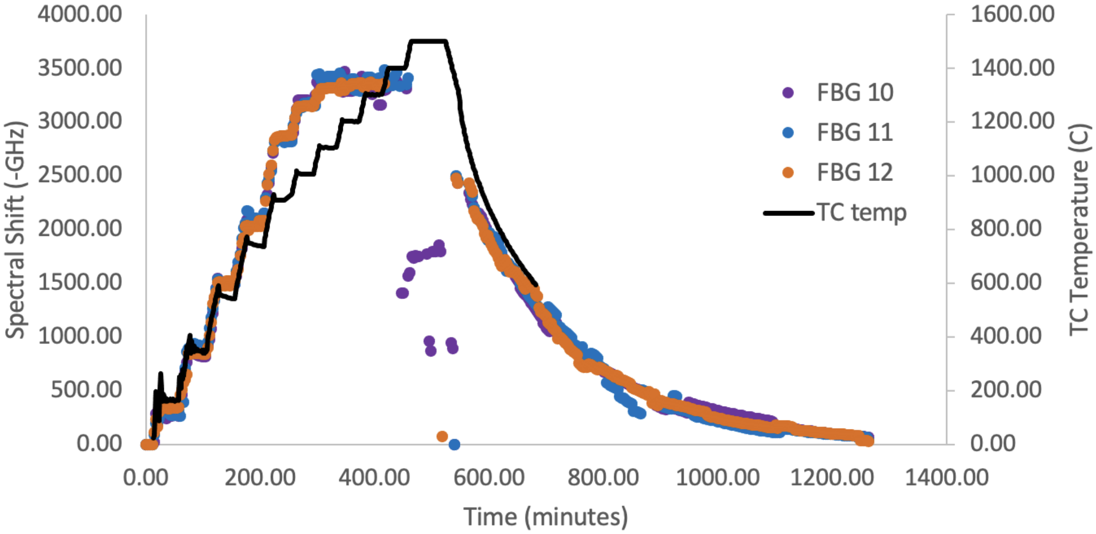

Figure 2. Response of sensor #1 during the out-of-core heating.

Figure 3 and Figure 4 show the backscatter profiles of the sensors before, during, and after the heating from room temperature up to 1200℃ and 1500℃, respectively. Because the thermal expansion of sapphire is significantly larger than that of silica, the FBGs being referenced by the interrogator to calculate the spectral shift have moved out of the range of the swept laser. This is confirmed by the fact that when the fiber cools, the sensing mechanism recovers. It is also confirmed by looking at individual scans of the fiber in the frequency domain and backscatter profile. Figure 5 and Figure 6 show the peak wavelength of FBG #12 moving out of the interrogator's range as it is heated, then back into the measurement range as it cools. Note that at 1100℃ and above, a significant reduction occurs in the amplitude of the FBGs. This reduction vanishes when the fiber cools. Previous research showed that an aluminum hydroxide formed on the surface of the optical fibers when they were heated to 1300℃ or above. [7] The fibers in the present work were sealed within the alumina tubes so as to limit any oxygen exposure, and the internal cladding should have limited any surface-level effects. Additional testing on clad and unclad sapphire fibers with inscribed FBGs, using a laser with a larger wavelength range, is needed to fully evaluate the reason behind the temperature-dependent amplitude reduction.

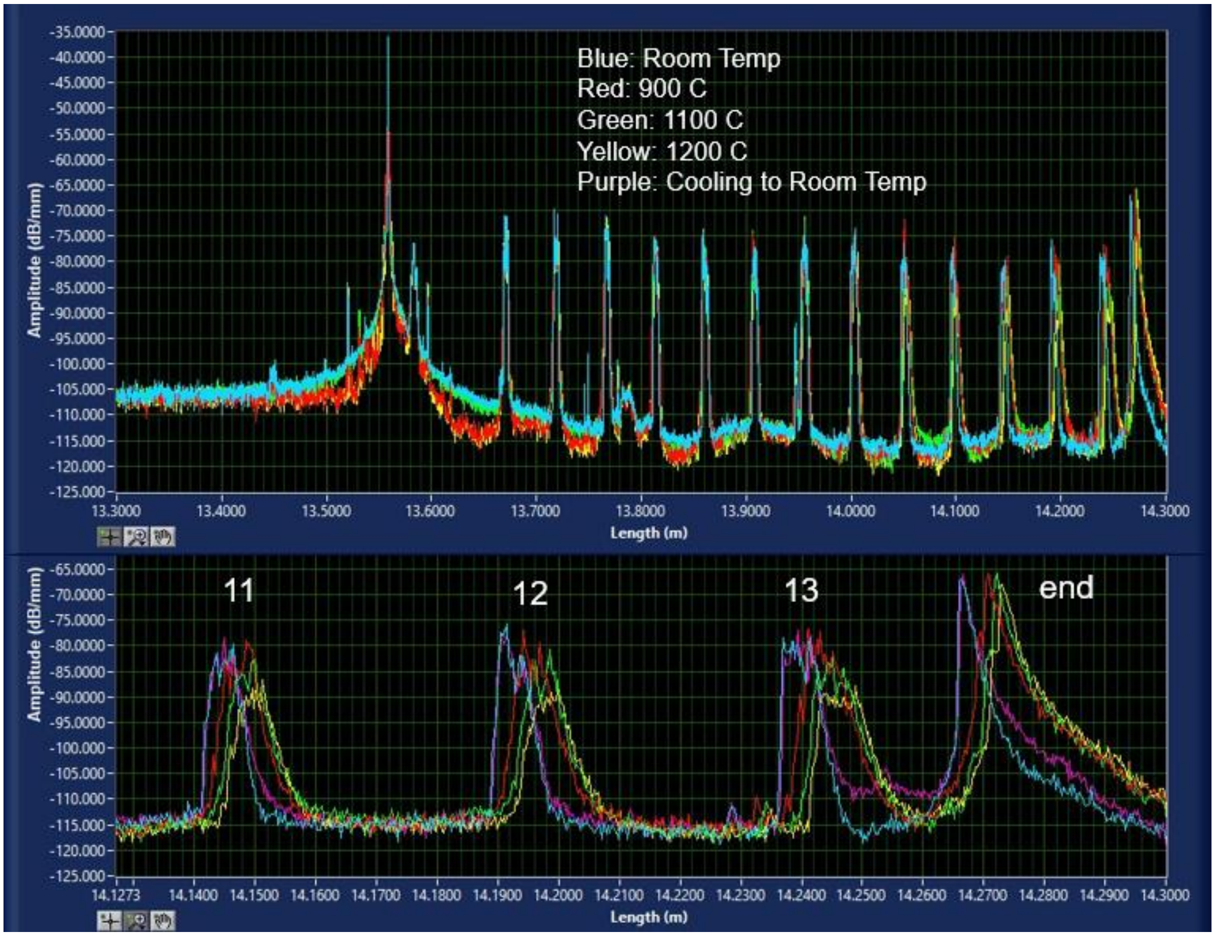

Figure 3. Top: Backscatter profile of sensor 1 before, during, and after the out-of-core heating from room temperature to 1200℃. Bottom: Top image zoomed in on the last three gratings in the fiber.

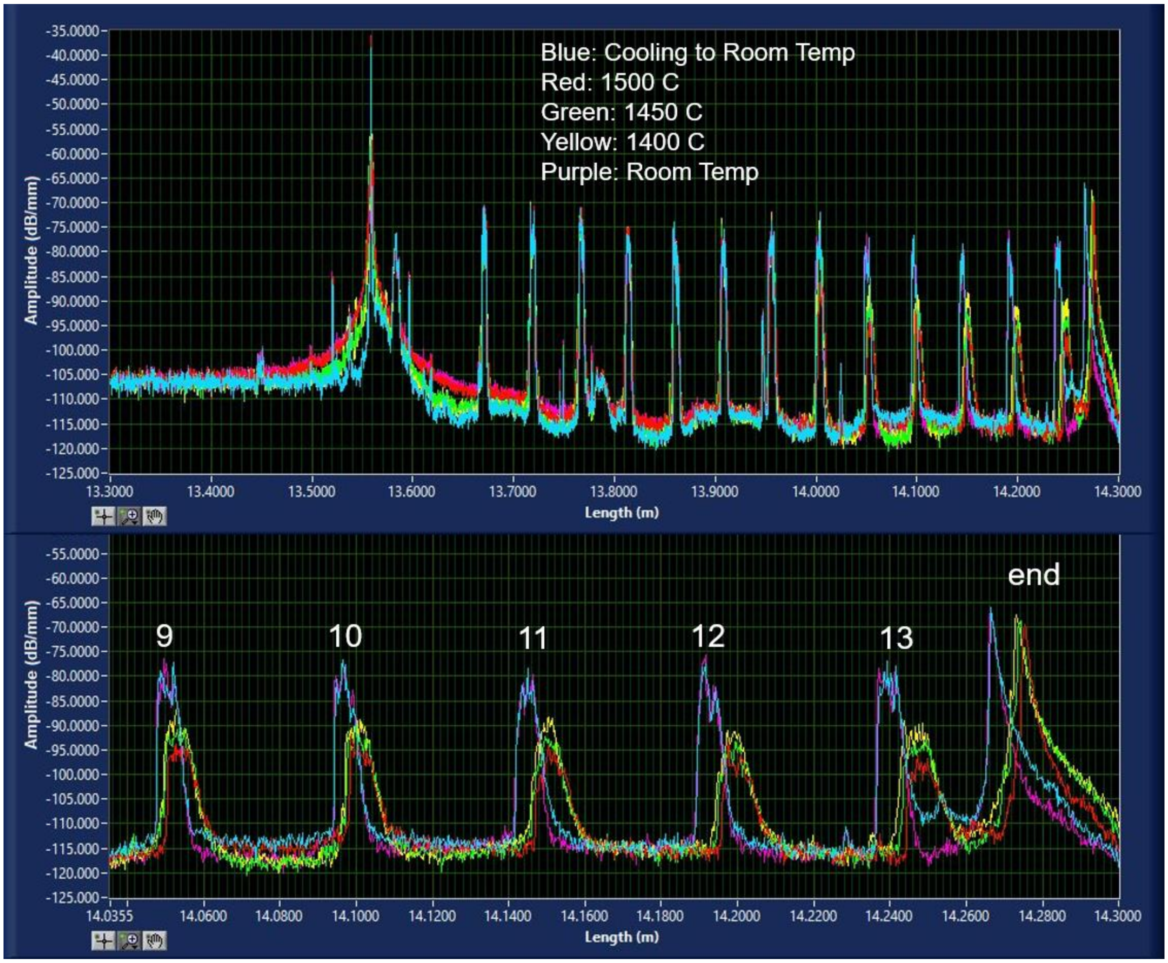

Figure 4. Top: Backscatter profile of sensor 1 before, during, and after the out-of-core heating from room temperature to 1500°C. Bottom: Top image zoomed in on the last three gratings in the fiber.

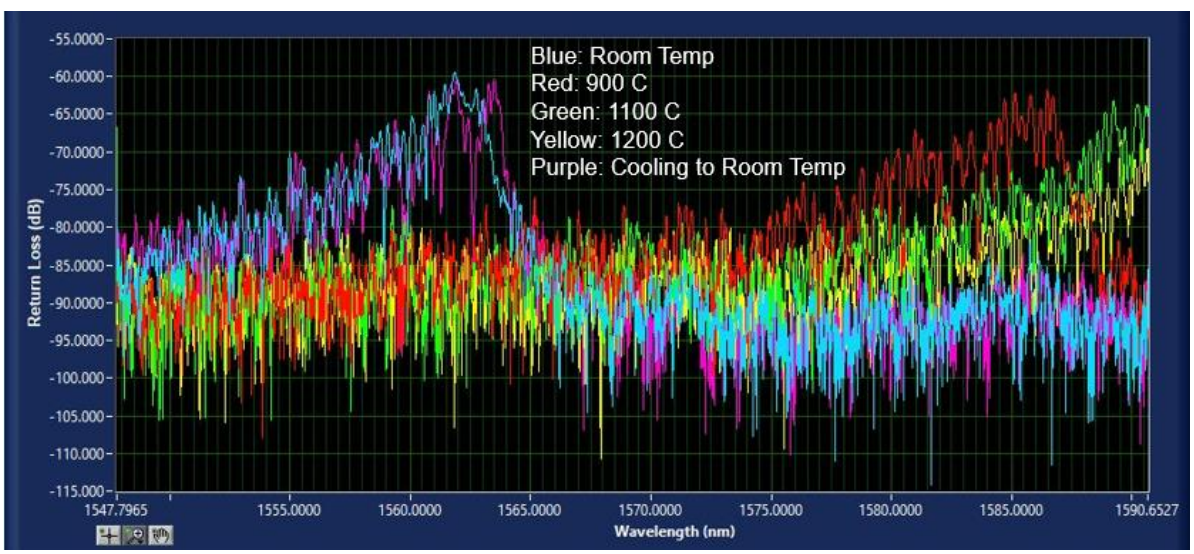

Figure 5. Frequency response of FBG #12 before, during, and after the out-of-core heating from room temperature to 1200°C.

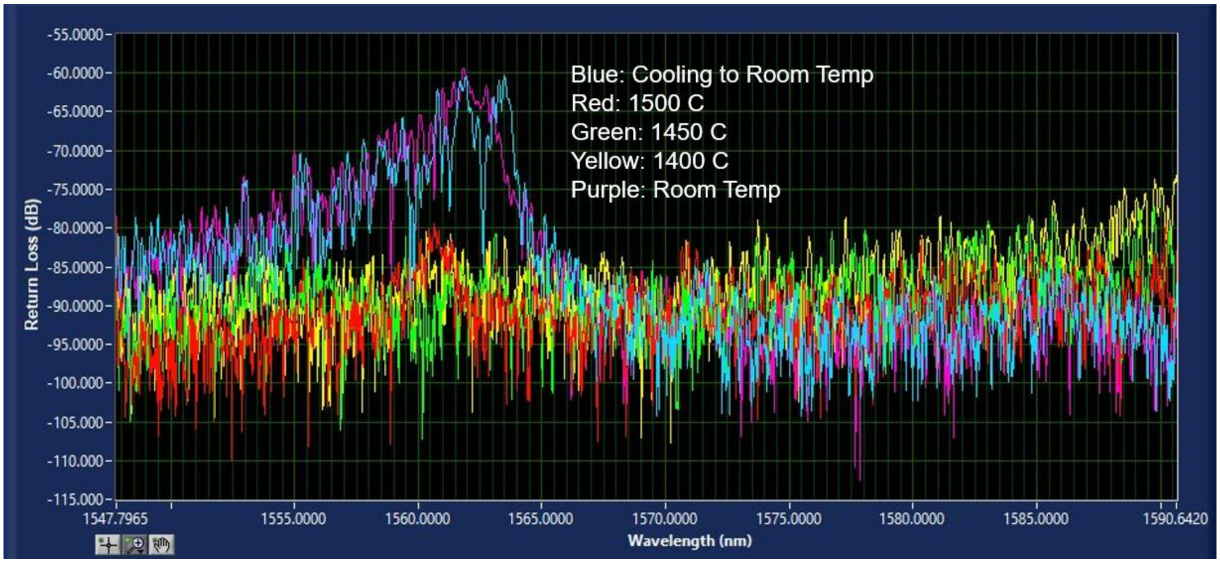

Figure 6. Frequency response of FBG #12 before, during, and after the out-of-core heating from room temperature to 1500°C.

4.3 Heated Irradiation Test

Eighty hours of irradiation in OSURR’s 10-in. dry tube was planned in order to test the combined effects of irradiation and temperature on the sapphire fiber sensors. The fibers would be heated up to 1600°C while under irradiation.

4.3.1 Rig Design and Assembly

In total, seven sensors were prepared for the heated irradiation at OSURR: five sapphire optical fiber sensors and two silica optical fiber sensors. All the sensors were packaged into 99.5% alumina tubes that were closed on one end (i.e., the end to be inserted into the furnace). The "tubes were then transferred into a flexible stainless-steel tubing and terminated using a fiber-optic connector angled physical connection (FC/APC) connection. Figure 7 shows the packaging used for all the fibers throughout the irradiation. The sapphire fibers were all spliced to pure silica core, fluorine-doped clad, single-mode silica optical fiber before leaving the alumina tube. All seven fibers and three Type B thermocouples were placed in the furnace rig provided at OSURR, via an alumina plug.

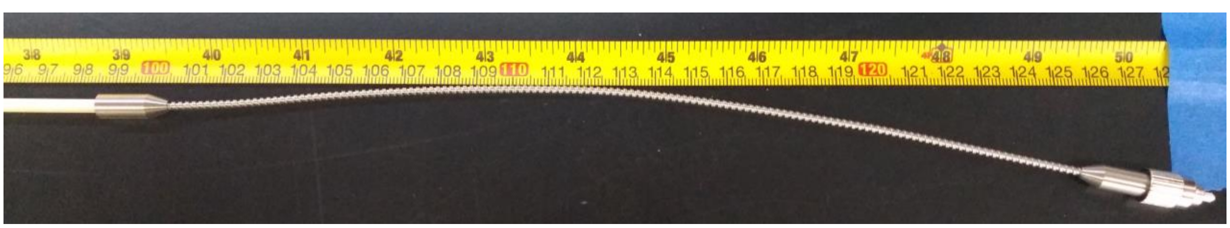

Figure 7. Fiber packaging for the OSURR heated irradiation.

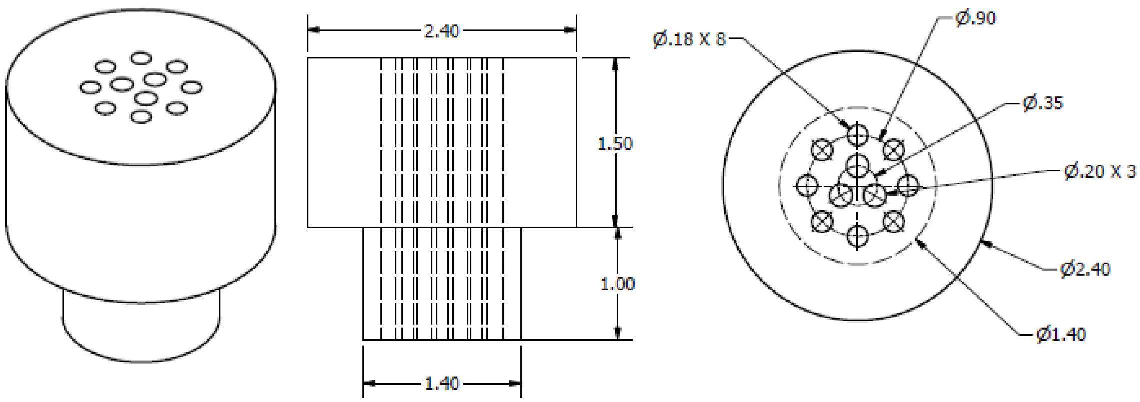

Figure 8. Alumina cap for the heated irradiation furnace rig (units are in inches).

The furnace consisted of four u-shaped $MoSi_2$ heating elements surrounded by insulation. The furnace had a 1.5-in.-diameter opening and a 12-in.-long heated region. The furnace was placed into an aluminum rig for lowering it into the 10 in. dry tube at OSURR. The fibers and thermocouples were placed into the furnace via the alumina cap and strain relieved at the top of the rig. The fibers were then connected to 30-ft-long SMF-28 optical fiber jumper cables to connect them back to the Luna OBR 4600. The fibers were positioned so as to keep the sapphire-to-silica splices out of the heated region, and the thermocouples were placed at the top, center, and bottom of the heated region in the furnace.

Figure 9. Furnace rig with the fiber sensors and thermocouples installed, ready for insertion into OSURR.

4.3.2 Irradiation and Results

From March 26 to April 21, 2021, the sapphire and silica optical fiber sensors were irradiated at OSURR for a total of 80 hours at 450 kW in a furnace, with temperatures varying from ambient up to 1600℃. All the sensors were packaged as mentioned in the previous section. Table 3 lists the different sensors, along with details on the pretreatment. The irradiation schedule and the temperatures achieved are shown in Table 4.

Table 3. Optical fiber sensors irradiated at OSURR.

#	Name	OD (um)	Length (in.)	Clad	Anneal Temperature ℃	No. of FBGs	FBG manufacturer	Notes
1	75um	75	23.5	yes	1500	13	FemtoFiberTec.	Mode Stripping
2	1120	100	13	yes	1500	2	U. Pitt.	Mode Stripping
3	D	100	15.25	yes	1200	1	U. Pitt.	Mode Stripping
4	Bare	100	9.25	yes	1500	0	N/A	Mode Stripping
5	C	100	16.25	yes	1500	1	U. Pitt.	Mode Stripping
6	iX Blue	125	24	N/A - silica fiber	N/A	0	N/A	Coating Removed
7	SMF-28	125	24	N/A - silica fiber	N/A	6	FemtoFiberTec	Coating Removed

Table 4. Irradiation and heating schedule.

Date	Rx Run (y/n)	Hours	Power (kW)	Furnace Temp. (℃)	Notes
3/22/2021	N	0	0	0	Setup
3/23/2021	N	0	0	0	Setup
3/24/2021	N	0	0	0	Setup
3/25/2021	Y	?	5 kW, 40 kW, 100 kW	0	Other customer
3/26/2021	Y	7	450	half 0 half 200	(Extraction part 1)
3/29/2021	N	0		0	No operations
3/30/2021	Y	7	450	400/600	
3/31/2021	Y	7	450	800	
4/1/2021	Y	4/+?	450 kW / 5 kW	900	4 hours, some hours for another customer
4/2/2021	N	0			Fuse blow #1
4/5/2021	N	0			Troubleshooting furnace
4/6/2021	N	0			Troubleshooting furnace

4/7/2021	N	0			Troubleshooting furnace
4/8/2021	Y	?	5 kW, 40 kW, 100 kW	No heat	Other customer
4/9/2021	Y	7	450	1000	
4/12/2021	Y	7	450	1100	
4/13/2021	Y	7	450	1200	
4/14/2021	Y	7	450	1300	
4/15/2021	Y	0	5 kW, 250 kW	No heat	Other customer
4/16/2021	Y	7	450	1400	
4/19/2021	Y	7	450	1.5 hr 800, 2 hr 1000, 2 hr 1200	
4/20/2021	Y	7	450	1 hr 1400, 6 hr 1500	Fuse blow during heating
4/21/2021	Y	6	450	1 hr 1500, 6 hr 1600	

Sensor 1 performed the best of the five sapphire sensors tested, likely due to the more distinct nature of the commercially inscribed FBGs as compared to those inscribed by an experimental entity. The smaller diameter of the fiber may also play a part in its performance. In this method, the cladding depth is limited by the available energy for the tritons and alphas to implant in the fiber. A fiber with a smaller overall diameter results in a smaller effective core region and could produce a more single-mode type of performance. This would improve the accuracy of the OFDR sensing used to evaluate the fibers in this test. Figure 10 shows the backscatter profile of sensor 1; the top of the furnace is located at 13.85 m and the bottom is located at 14.3 m with respect to the fiber.

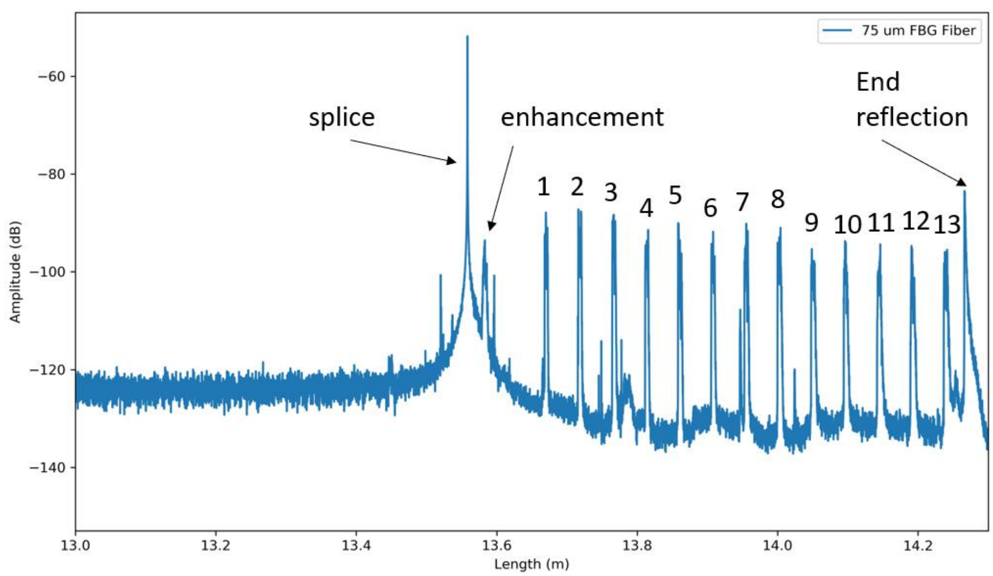

Figure 10. Backscatter profile of sensor 1, a 75-um-OD sapphire fiber with FBGs from FemtoFiberTec.

Figure 11 and Figure 12 show the response of sensor 1 on day 1 for 3.5 hours with the furnace off, 3.5 hours with the furnace at 200℃, and with reactor power at 450 kW for the full 7 hours. Figure 11 shows the response at the FBG locations; Figure 12 shows the response along the length of the fiber. The OFDR sensing cannot reference the fiber’s backscatter profile in between the FBG locations; however, it successfully references it at the FBG locations. The fiber responds very well to the temperatures, and returns to room temperature when the furnace and reactor are off.

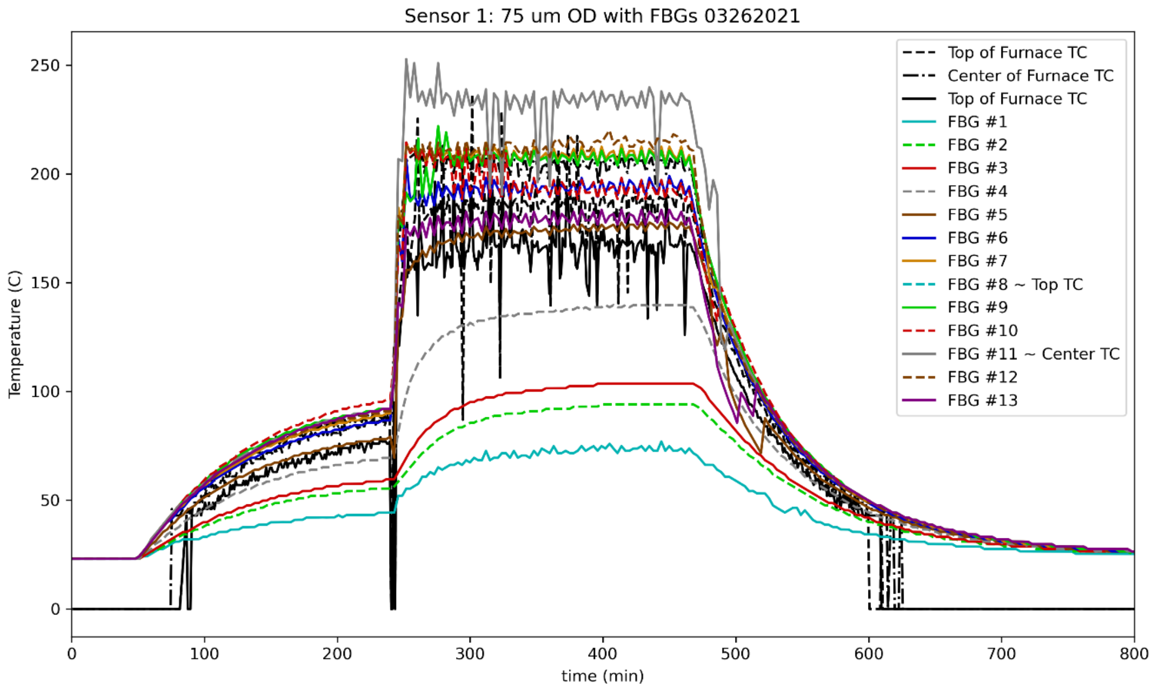

Figure 11. Temperature response at the FBG locations of sensor 1 over time: day 1 of the irradiation.

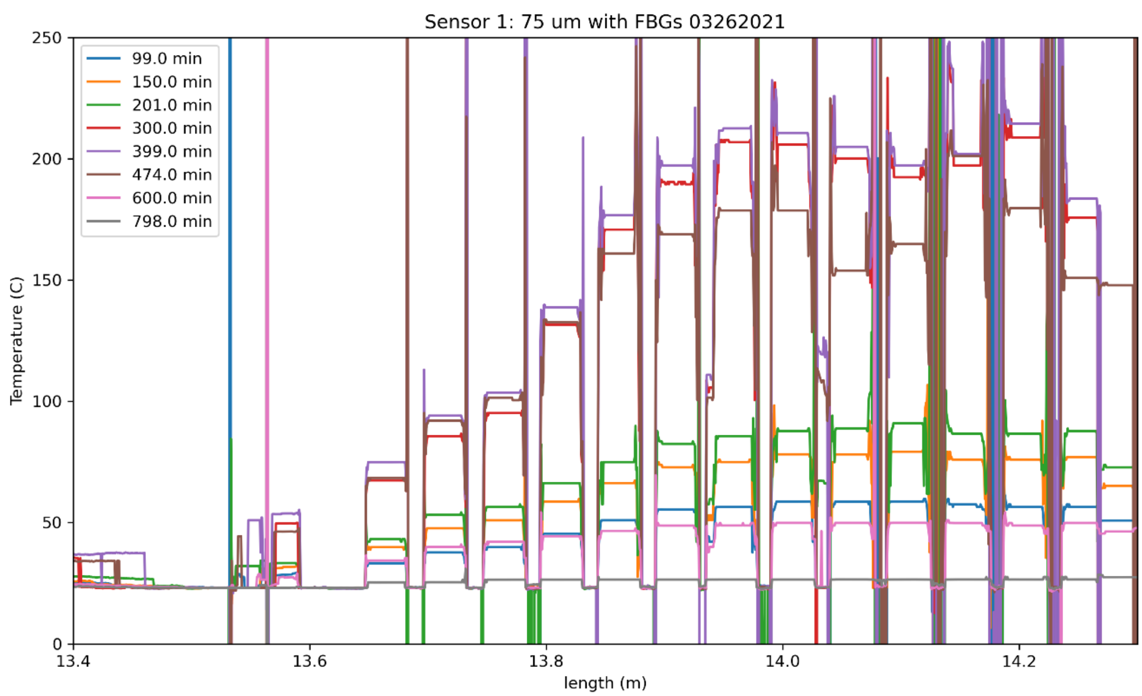

Figure 12. Temperature response of sensor 1 along the length of the fiber for various times during day 1.

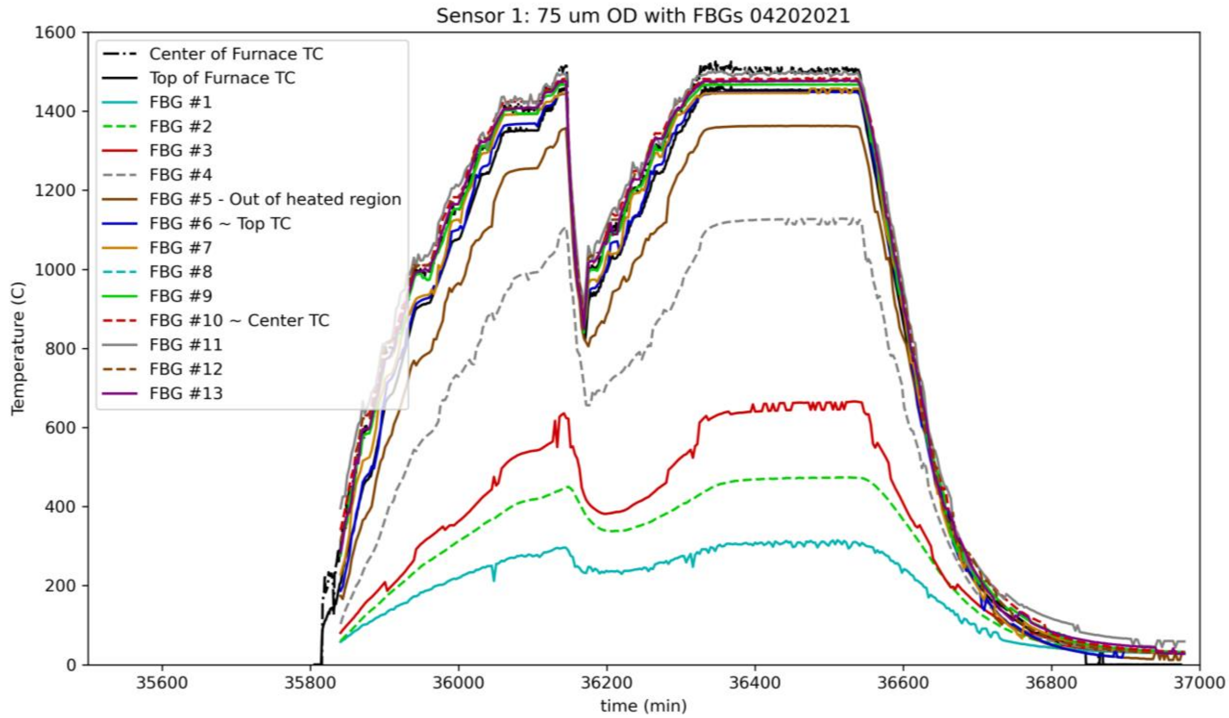

Figure 13. Sensor 1 response on day 11 for 1 hour at 1400℃, followed by an unexpected fuse blow, reheat, and then 5 hours at 1500℃, with the reactor power at 450 kW.

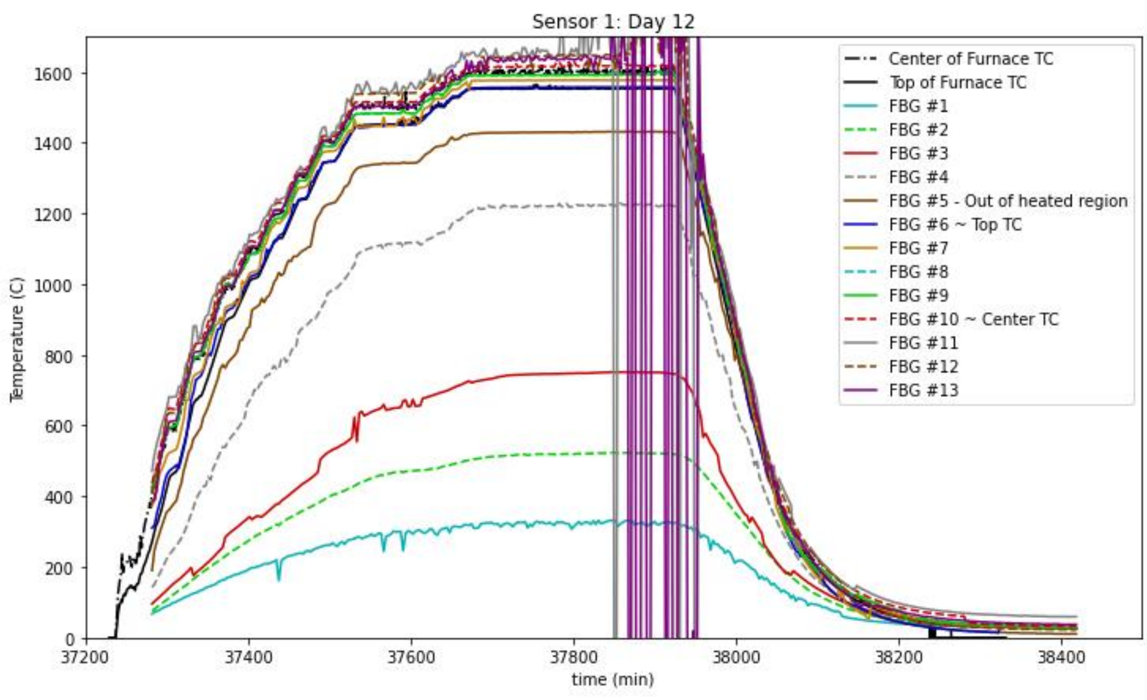

Figure 14. Sensor 1 response on the final day, day 12, for 1 hour at 1500℃ and 5 hours at 1600℃, with the reactor power at 450 kW.

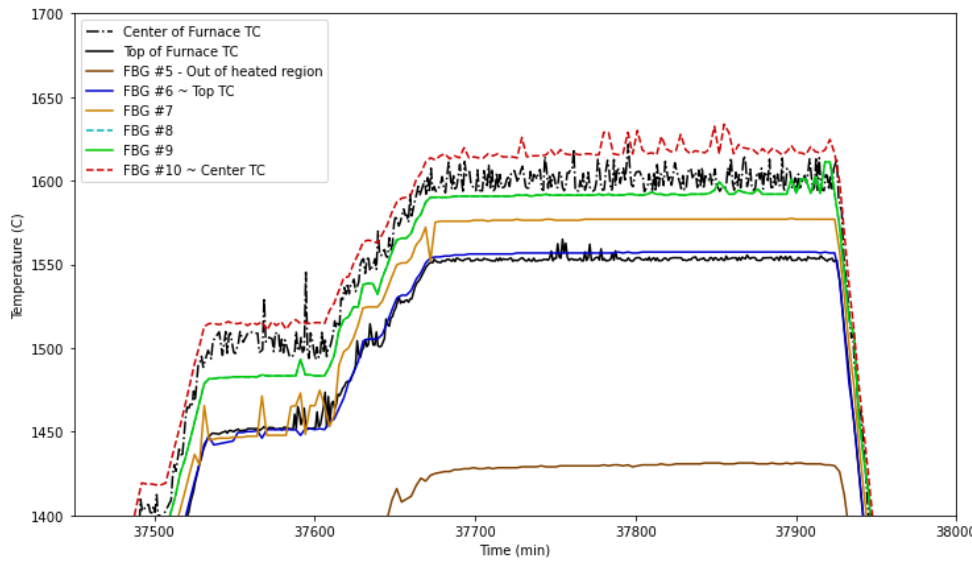

Figure 15. Sensor 1 response at temperature holds on the final day, day 12, for 1 hour at 1500°C and 5 hours at 1600°C, with the reactor power at 450 kW. Note that the failed FBGs have been removed.

Figure 13 and Figure 14 show the last two days of the irradation, which were the days when the furnace was hottest. Figure 13 shows the FBGs in the fiber reading the temperature very well, including an unexpected thermal transient due to a blown fuse in the furnace. The furnace was then reheated and held at 1500°C for the remainder of the irradation, and the reactor was held at 450 kW for the rest of the day. On the last day, the irradiation was conducted at 1600°C, with a 1500°C 1-hour soak. The response of sensor 1 is shown in Figure 14 and Figure 15. Figure 14 reflects a failure of referencing in FBGs #11, #12, and #13—the three FBGs with the longest transmission in the sapphire fiber. Figure 15 shows sensor 1's response (without the failed FBGs) during the high-temperature holds. The close-up reveals some noise in the measurement, but no more than what occurs in the Type B thermocouple. FBG #6 is positioned at approximately the location of the top thermocouple and is reading a steady, accurate temperature. FBG #10 is positioned approximately at the location of the Type B thermocouple at the midplane of the furnace. This FBG contains some noise in its signal, but less than the conventional thermocoule.

Sensor 2 recorded an interesting phenomenon observed in the furnace testing (i.e., a flattening of the sepectral shift change that does not correlate to temperature), as seen in Figure 16. This occurs at the same temperature (i.e., just above 1500°C) as it did in the out-of-pile furnace testing.

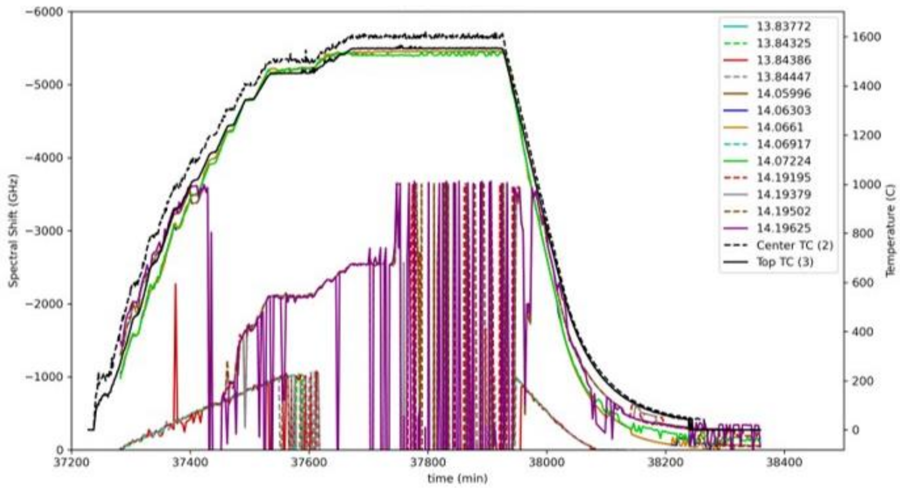

Figure 16. Sensor 2 response on the final day, day 12, for 1 hour at 1500°C and 5 hours at 1600°C, with the reactor power at 450 kW.

Figure 18 shows, for sensor 1, the backscatter profile and wavelength response of FBG #12—the very initial response prior to any irradatiation (i.e., the reference scan)—after the second-to-last day at room temperature, at 1500°C and 1600°C on the last day, and then cooled to nearly room temperature after the last day. The out-of-core testing saw this failure at 1200°C (rather than at 1600°C, as seen here) because adjustments were made to the interrogater in order to widen the wavelength range. The failure at 1600°C appears to stem from a complete loss of reflected amplitude in the fiber. The FBG amplitudes reduce with temperature and time; however, when the fiber returns to room temperature, the amplitude recovers to the same amplitude observed prior to the heating/irradation. **Error! Reference source not found.**shows the b ackscatter profile and wavelength response of FBG #12 as the fiber cools down from 1600°C. As seen, the amplitude recovers as the fiber cools.

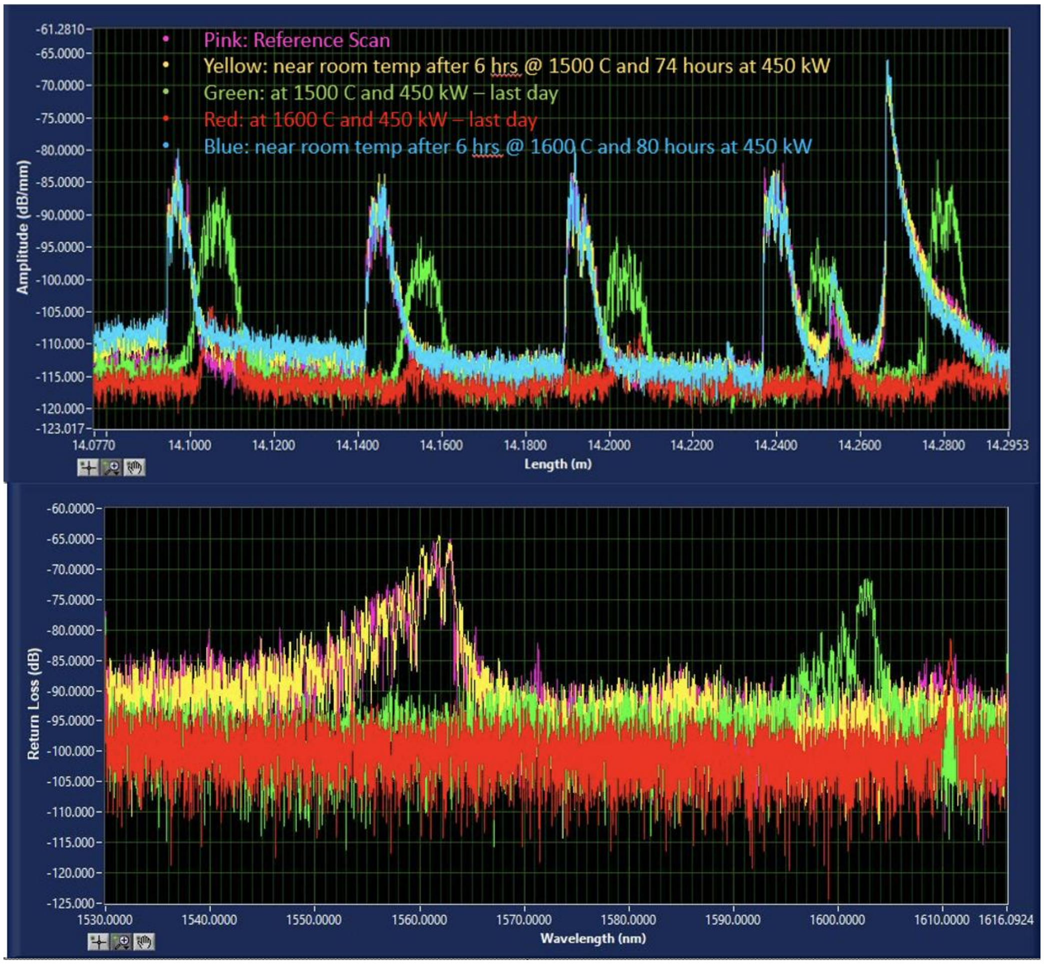

Figure 17. (Top) Backscatter profile and (Bottom) wavelength response of sensor 1's FBG #12 during the last day of irradiation heating.

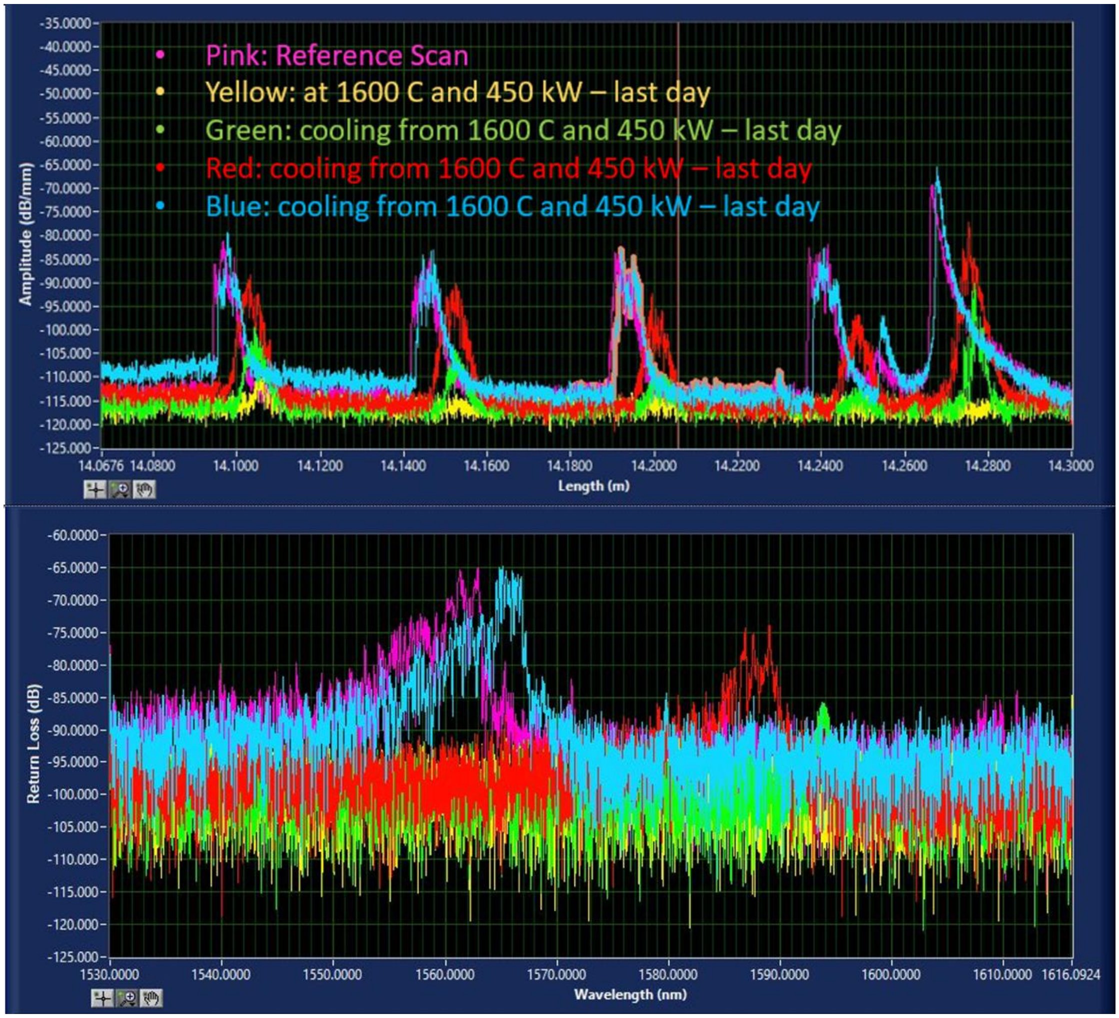

Figure 18. (Top) Backscatter profile and (Bottom) wavelength response of sensor 1's FBG #12 during the last day of irradiaiton cooling.

Further investigation is necessary to detemine the cause of this time- and temperature-dependent amplitude reduction in the fibers. Non-clad FBG inscribed fibers were shown to respond well at up to 1900°C, indicating that the attenuatuin mechanism may be an effect caused by the damage layer of the cladding. The sensor showed little to no drift or attenuation once returned to room temperature after 80 hours at 450 kW (approximately 2.9 x 10^{17} n/cm^2 total fluence, from a total flux of 10^{12} n/cm^2/s). [8] The sapphire sensor outperformed the Type B thermocouples, providing a stable temperature reading with less noise than when using the thermocouples. This is a promising indication that sapphire optical fibers can be used for ultra-high-temperature reactor experiments. However, it is essential that defect structures are inscribed in the fibers and that the appropriate thermal annealing is conducted prior to sensor deployment.

5. RESULTS OF THE HIGH-FLUENCE IRRADIATION AT MIT

5.1 Test Matrix

Five sapphire and three silica fibers were irradiated at MIT. The silica fibers were included as a basis for comparison, as they have been extensively studied in terms of irradiation use. The test matrix is described in **Error! Reference source not found.**. The sapphire fibers were all spliced to pure silica core, s ingle-mode optical fiber lead-outs, and all were clad via the Li-6 enriched lithium carbonate irradiation method. After being clad, the fibers were thermally annealed to 1500°C in air, then spot-treated using a proprietary experimental mode-stripping treatment. Previous work indicated that chemical interactions with the sapphire fiber may cause attenuation. To reduce the possibility of the sapphire interacting with the stainless-steel capillary tubes, all the sapphire fibers were also placed in silica microcapillary tubes. A schematic of the sensor design is shown in **Error! Reference source not found.**. The silica capillary tube w as fused closed at the distal end of the sensor and epoxied at the top end. The epoxy was expected to degrade over the course of the irradiation. When the epoxy failed, if the capillary tube managed to move at all, it could only drop a maximum of 0.5 in. to the bottom of the stainless-steel tube. The epoxy at the top of the capillary tube was primarily intended to keep the tube in place during shipping and installation.

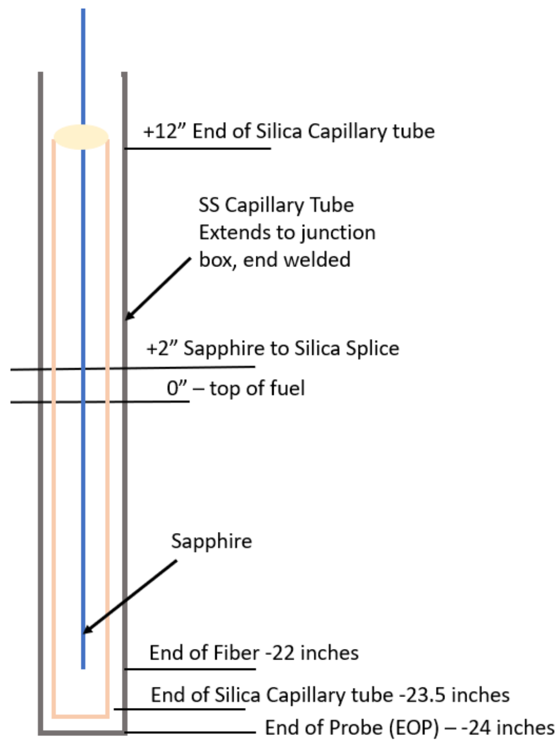

Figure 19. Optical fiber sensor probe design.

Table 5. MIT irradiation test matrix.

Sample Number	Description	MIT Designation	End of Sapphire (in.)*	Start of Sapphire (in.)*
1	Al_2O_3-75-1	FT1	12	26
2	Al_2O_3-100-1	FT2	9.5	26
3	Al_2O_3-100-2	FT3	15	29
4	Al_2O_3-125-1	FT4	4	26
5	Al_2O_3-125-2	FT5	14	26
6	Dead-End Silica	FT6	N/A	N/A
7	SiO_2-FBG-1	FT7	N/A	N/A
8	SiO_2-FBG-1	FT8	N/A	N/A

*Measured from the end of the metal capillary tube (end of probe)

Error! Reference source not found. through **Error! Reference source not found.** show, in their pr e-installation condition, the five sapphire sensors utilized in the experiment. The sensors were interrogated using the Luna OBR 4600. Their backscatter profiles show the splices, end reflections, and gratings along the fiber lengths.

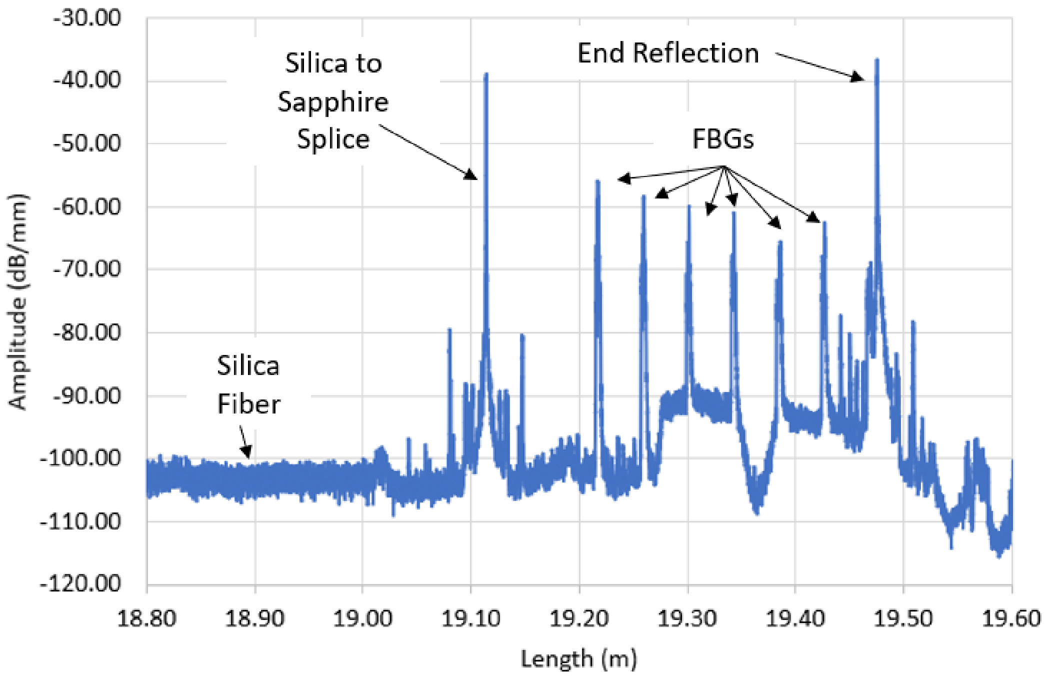

Figure 20. Sensor 1, 75 um in diameter, 14 in. long, with six FBGs inscribed by FemtoFiberTec, prior to installation in the experiment capsule.

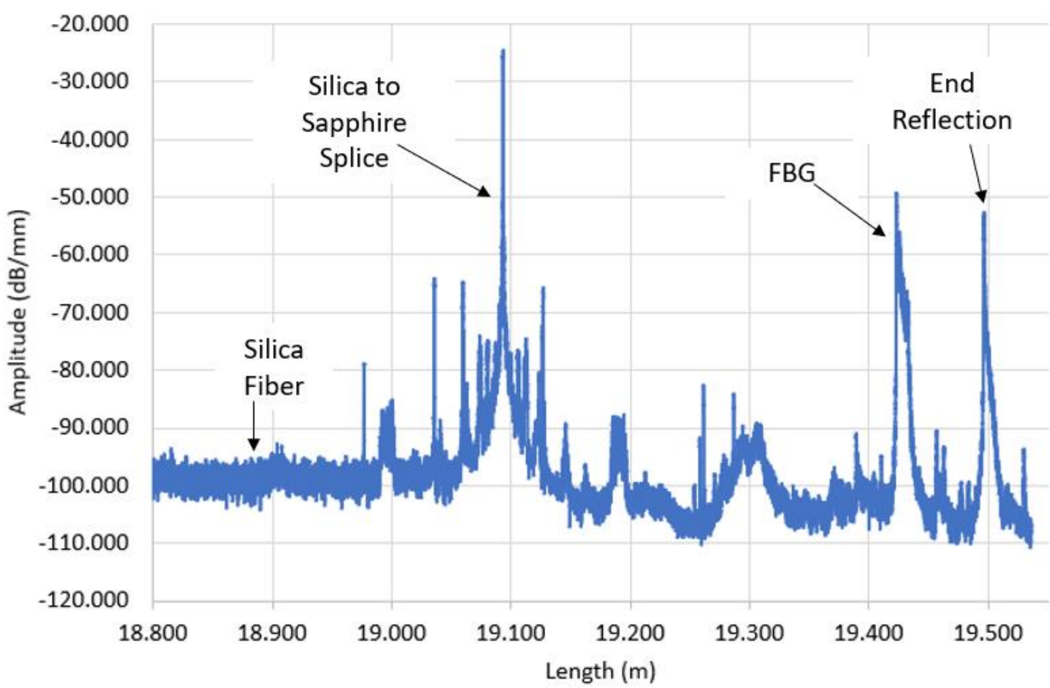

Figure 21. Sensor 2, 100 um in diameter, 16.5 in. long, with one FBG inscribed by U. Pitt, prior to installation in the experiment capsule.

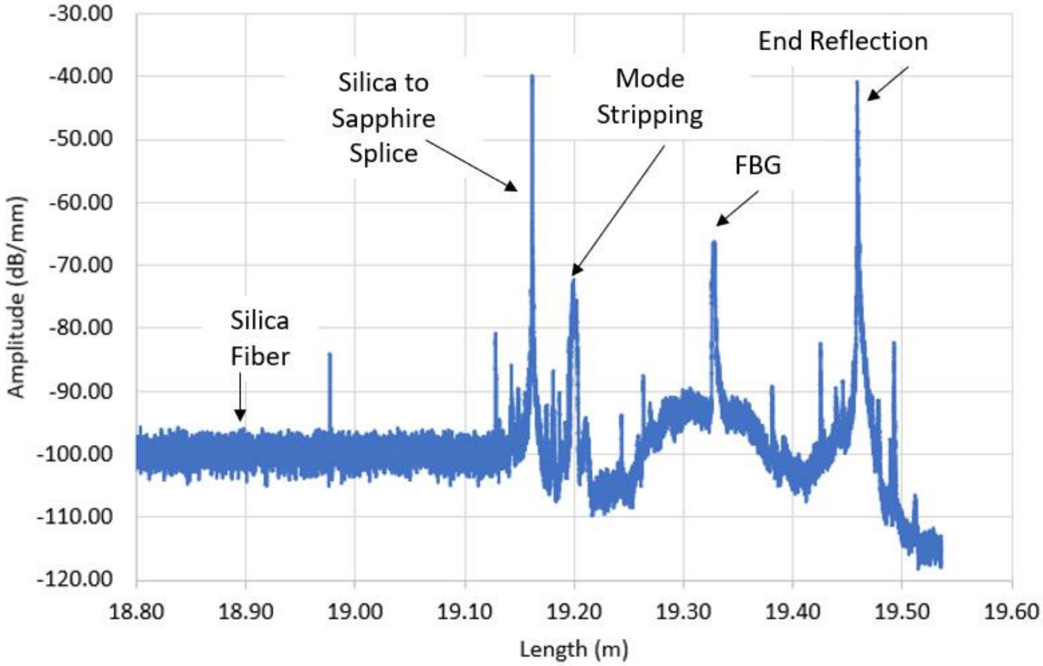

Figure 22. Sensor 3, 100 um in diameter, 14 in. long, with one FBG inscribed by U. Pitt, prior to installation in the experiment capsule.

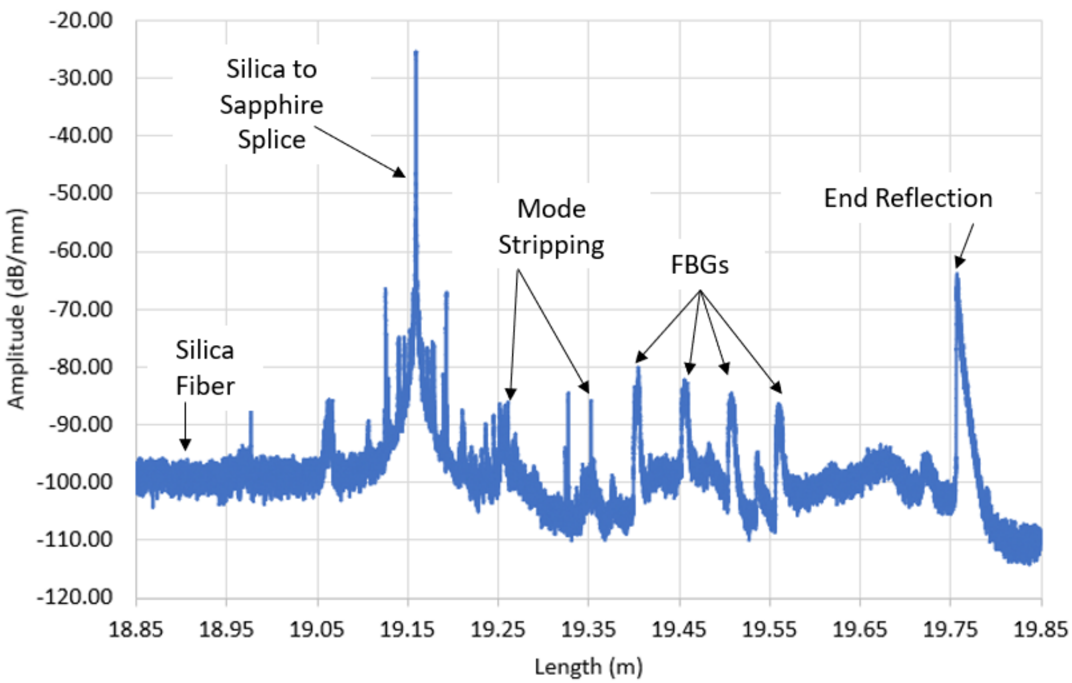

Figure 23. Sensor 4, 125 um, 22 in. long, with four FBGs inscribed by FemtoFiberTec, prior to installation in the experiment capsule.

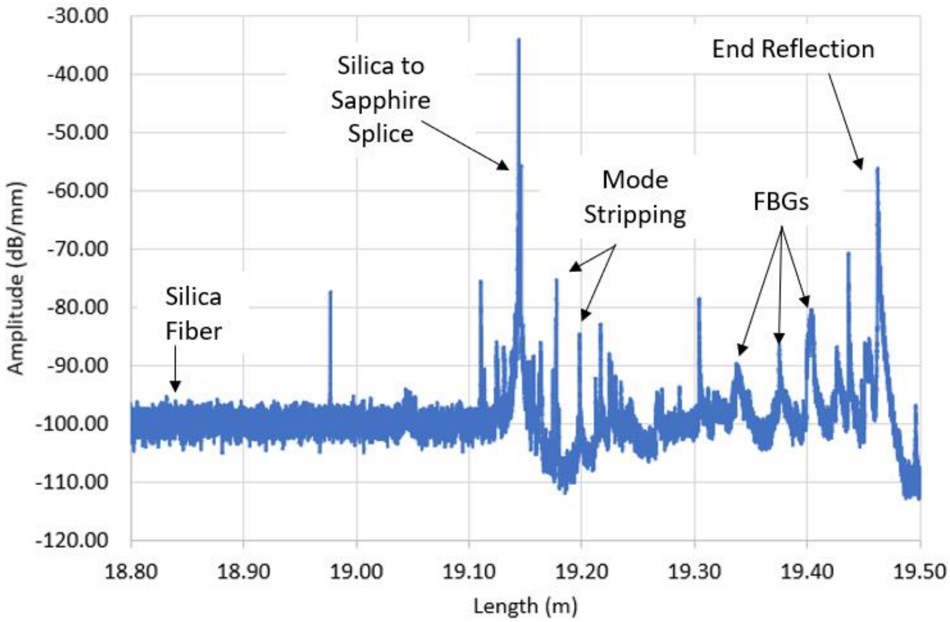

Figure 24. Sensor 5, 125 um, 12 in. long, with three FBGs inscribed by FemtoFiberTec, prior to installation in the experiment capsule.

5.2 Irradiation Rig Design

Irradiations were conducted in the core of the MITR, a research reactor whose maximum power capacity is 6 MW_{th}. The experiment was irradiated for two cycles in the MITR In-core Sample Assembly (ISCA), housed in the A-1 position within the core. The ISCA's position within the reactor is shown in Figure 25.

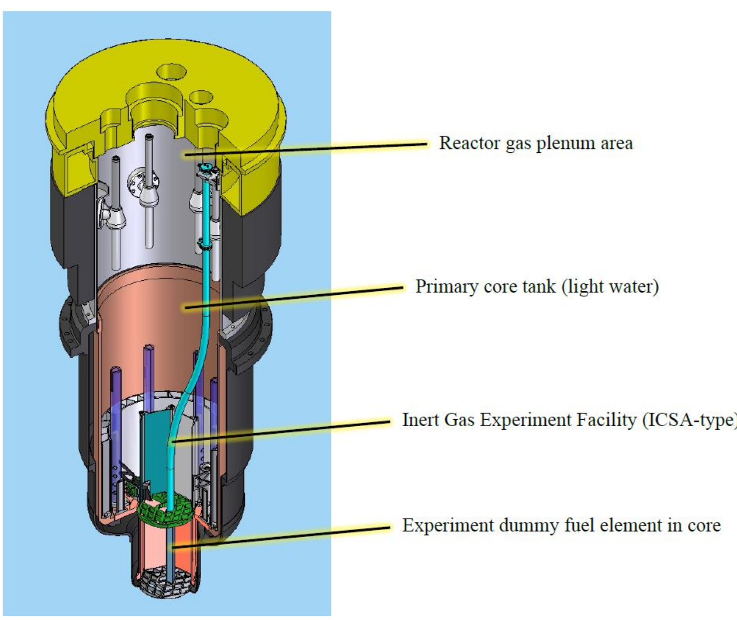

Figure 25. MITR schematic and ISCA position.

The A-1 position within the core is shown in Figure 26.

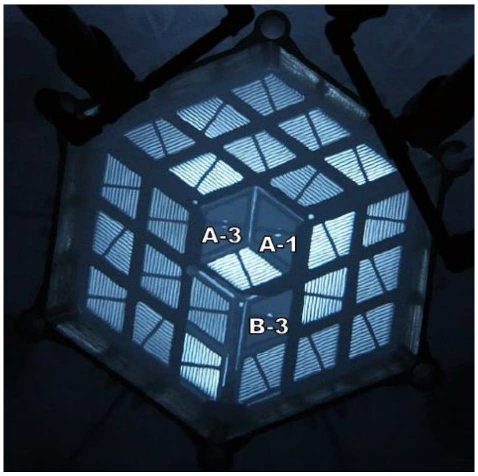

Figure 26. MITR core with three testing positions labeled.

The ISCA experiment vehicle is designed to replace one of the dummy fuel elements (for this experiment, A-1). The experiment rig is filled with inert gas, the composition of which may be changed to control the temperature. Temperatures for this experiment were nominally targeted at 600℃, with ramping cycles reaching as high as 750℃. The typical vehicle design, shown in Figure 27, consists of a cylindrical sample holder fit within a dummy tetrahedral fuel element.

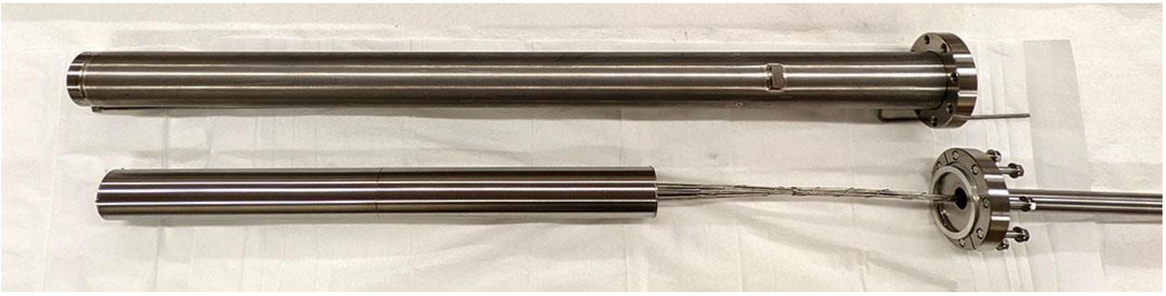

Figure 27. ISCA experiment vehicle.

Temperatures within the vehicle were monitored using four Type K thermocouples located at several positions along the length of the vehicle. These (approximate) positions are shown in Figure 28.

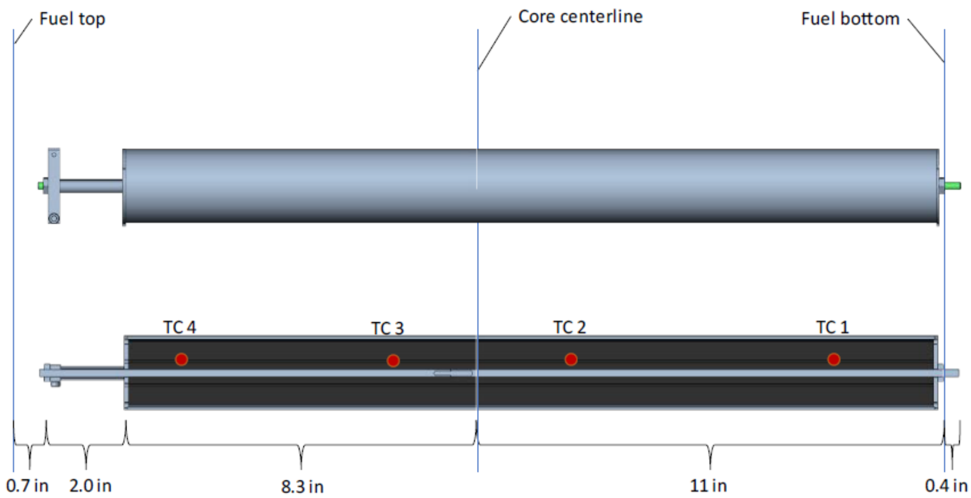

Figure 28. Experiment vehicle and the thermocouple locations.

5.3 Irradiation Results

The experiment reached a total fast fluence (>1 MeV) of $3.5 \times 10^{20}/cm^2$. Table 6 shows the total fluences for the neutrons and gamma dose. The reactor power and experiment thermocouple temperatures are shown at startup in Figure 29, for the entirety of cycle 1 in Figure 30, and for cycle 2 in Figure 31. The temperature during the test was around 680°C, as measured by TC#2, which was positioned just below the core center line. The temperature profile of the capsule was 550°C–680°C.

Table 6. Total fluence and dose achieved.

	Fluence ($1/cm^2$)	Exposure (MGy)
Total Neutron	1.6E+21	
Thermal Neutron (< 1 eV)	2.3E+20	
Fast Neutron (>0.1 MeV)	7.6E+20	
Fast Neutron (>1 MeV)	3.5E+20	
Gamma	1.6E+21	1.9E+04

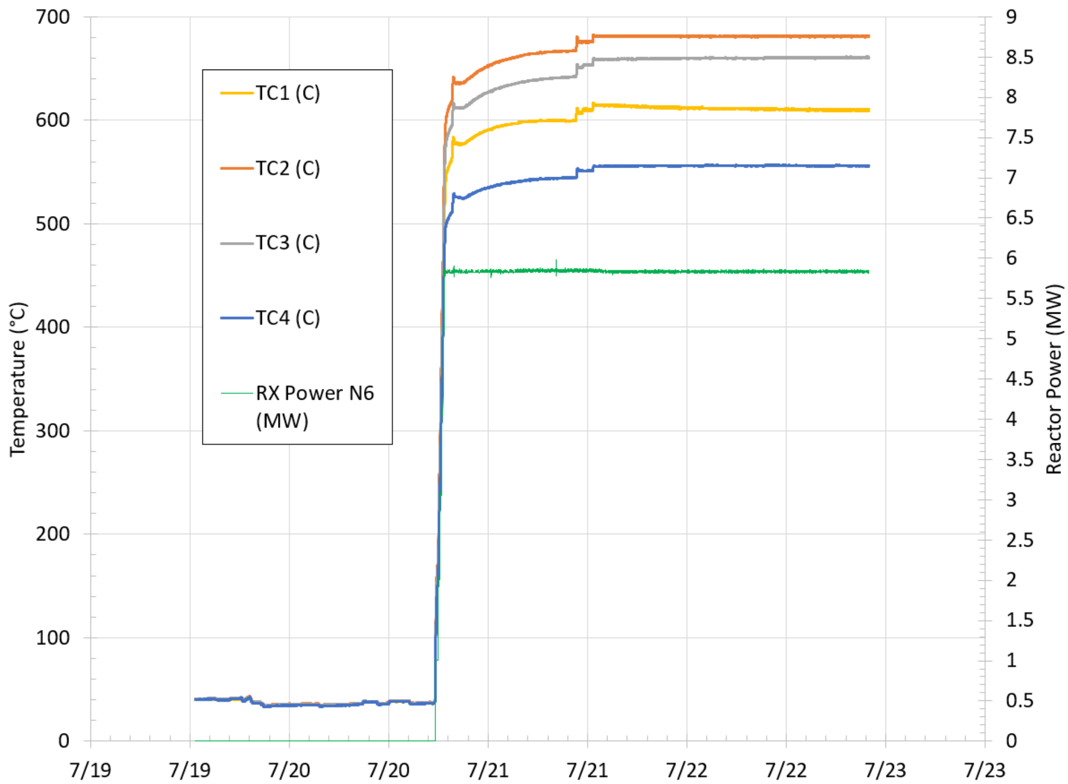

Figure 29. Reactor thermocouple temperatures and reactor power at startup.

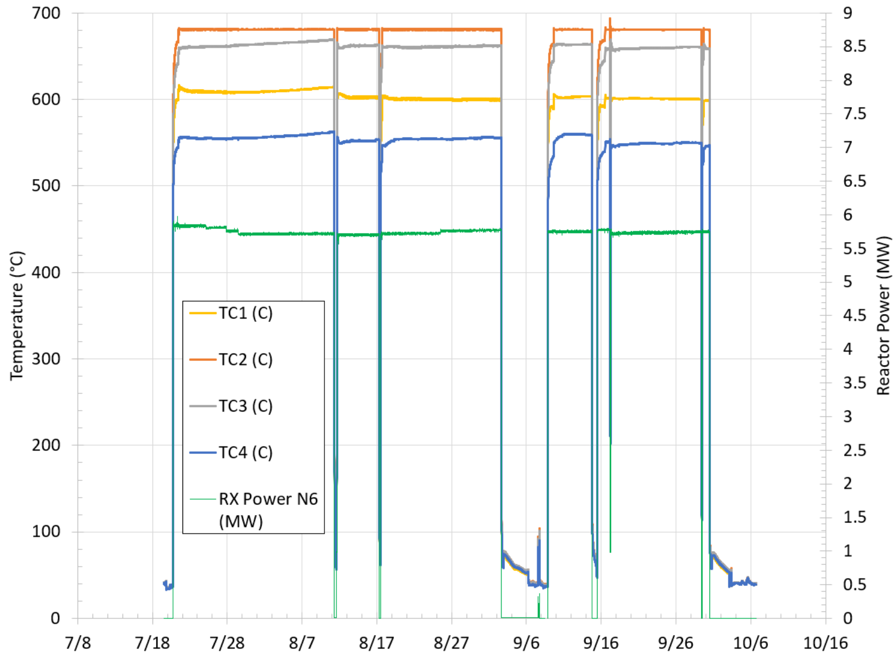

Figure 30. Cycle 1 thermocouple temperatures and reactor power.

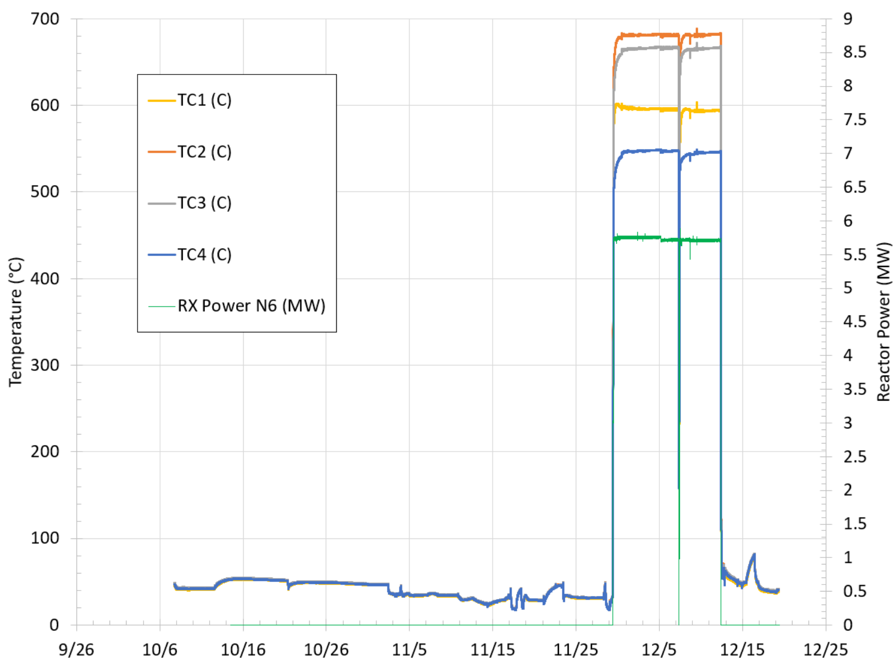

Figure 31. Cycle 2 thermocouple temperatures and reactor power.

The backscatter profiles of the sapphire sensors were monitored throughout the duration of the irradiation. Both sensors 1 and 2 were non-functional upon being installed in the reactor. Figure 32 and Figure 33 reflect the sensors just prior to reactor startup, as well as during the power ramp up to steady state over the first 2 hours of irradiation. Both sensors appear to experience significant reflections at the splice location. Sensor 1 does not appear completely fractured, as several scans over the first few hours appear to show light being transferred to the end of the fiber and back to the detectors. Even with a few full scans, sensors 1 and 2 are not useful for any type of performance evaluation, and will not be discussed further.

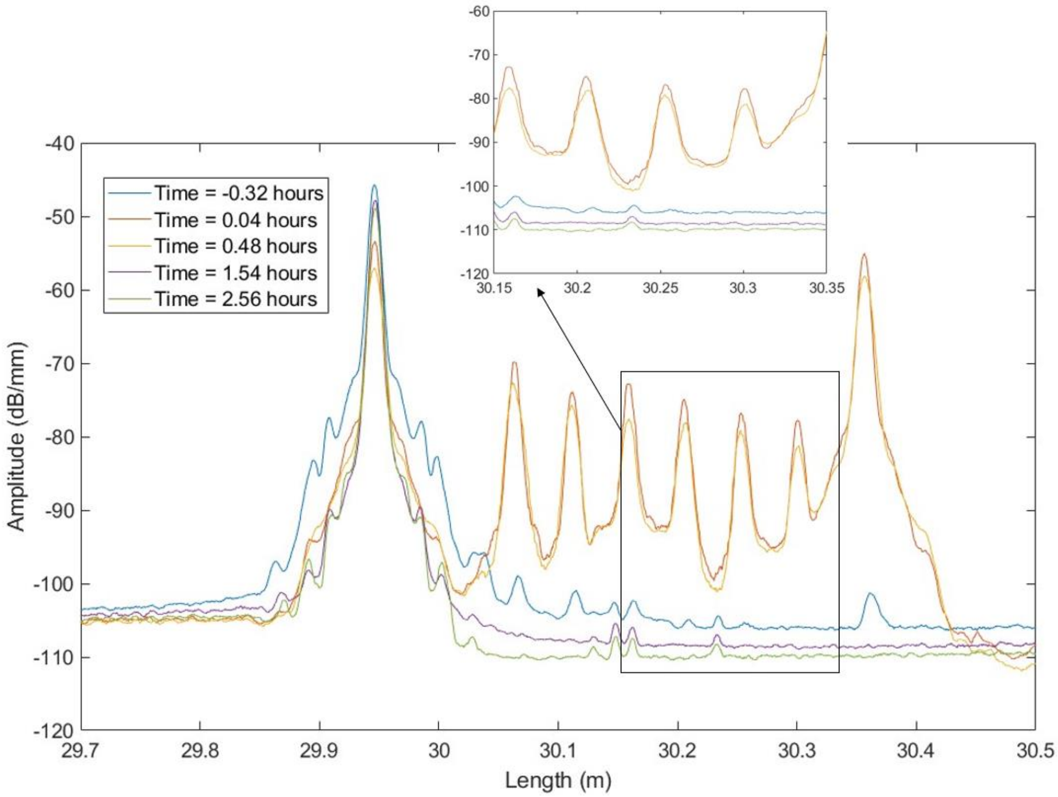

Figure 32. Sensor 1 during reactor initial startup for cycle 1.

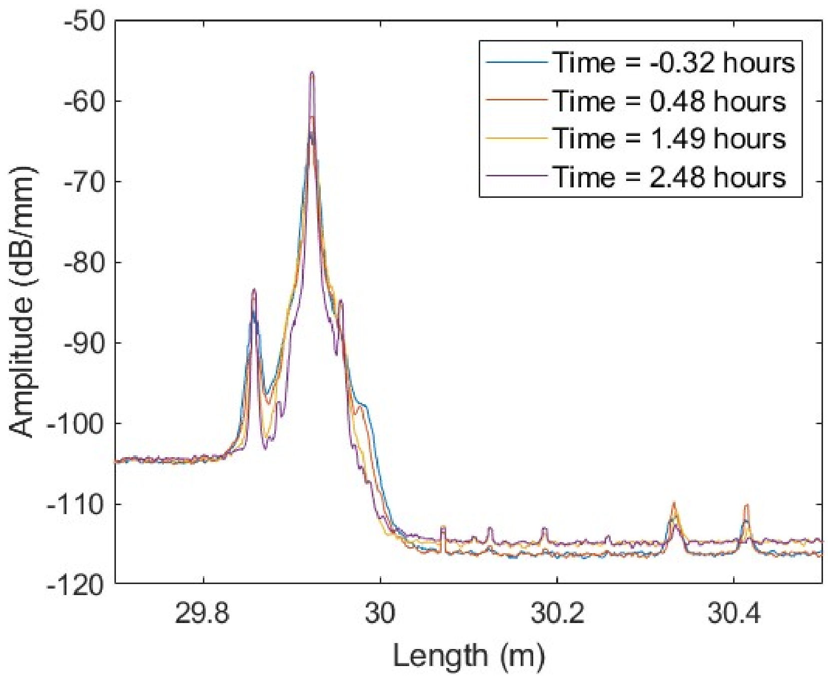

Figure 33. Sensor 2 during reactor initial startup for cycle 1.

Sensor 3 performed best of the five sapphire sensors. The backscatter profile for sensor 3 over the initial startup, and then for the first 35 hours at full steady-state power, are shown in Figure 34 and Figure 35, respectively. Over the first 35 hours, a reduction in backscatter amplitude occurs, possibly due to heating the fiber up to 680°C. Previous testing of clad sapphire sensors showed a temperature-dependent amplitude reduction that appears to level out after a few hours at steady-state operation. The FBG in sensor 3 is located near the top of the fuel region. The top of the fuel is at 30.15 m along the length of sensor 3.

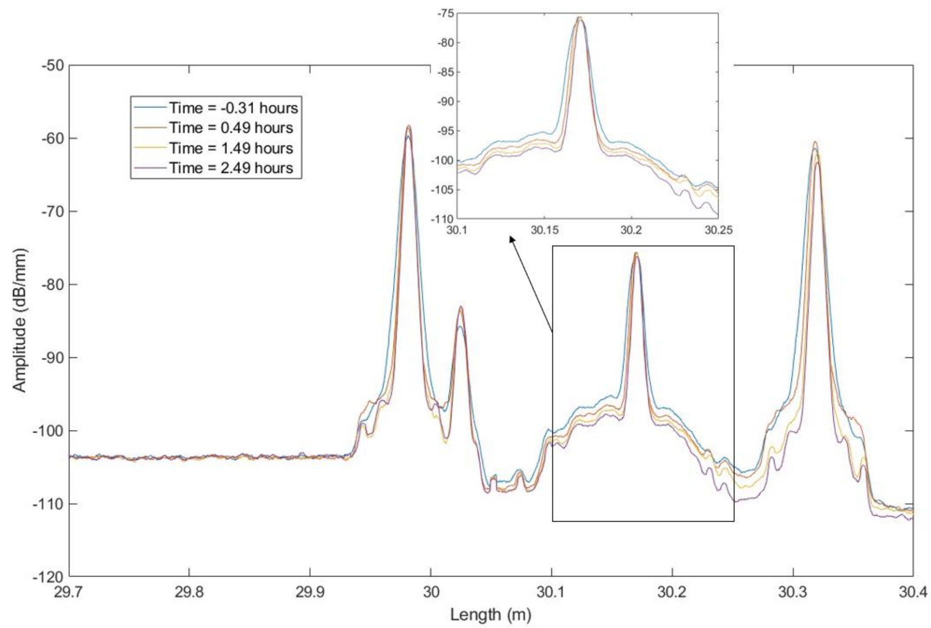

Figure 34. Sensor 3 during reactor initial startup for cycle 1.

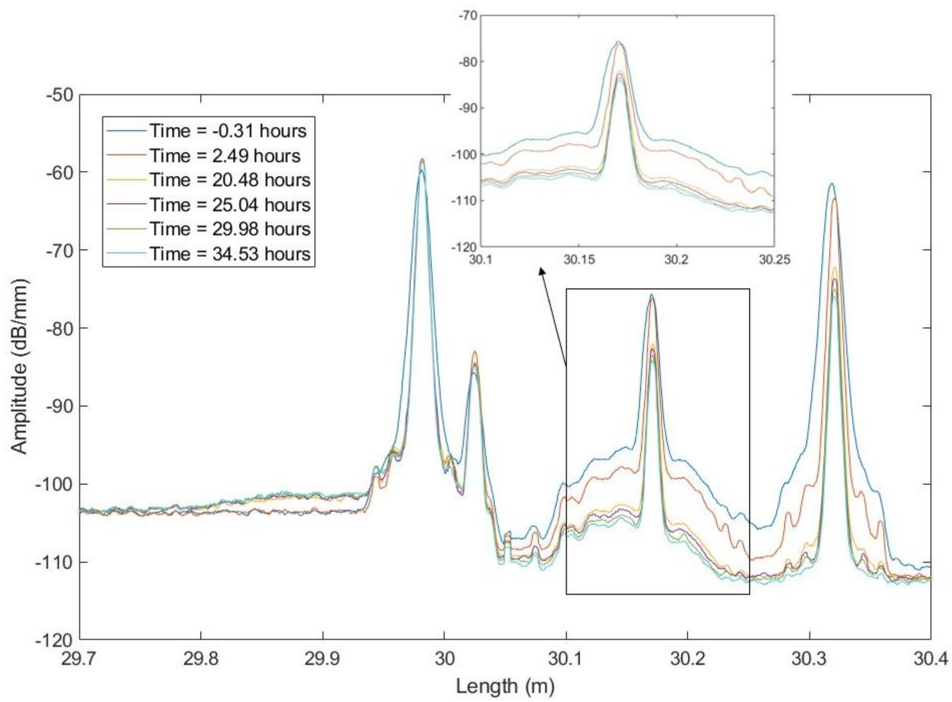

Figure 35. Sensor 3 during reactor initial steady state for cycle 1.

Figure 36 shows the backscatter profile of sensor 3 before, during, and after the two irradiation cycles. The increase in attenuation is significant. After the first irradiation cycle, the attenuation is such that the large reflection off the end of the fiber is no longer present. There is not enough light traveling down and being reflected back to the OBR. The FBG still reflects some light, but it is a significantly reduced amount.

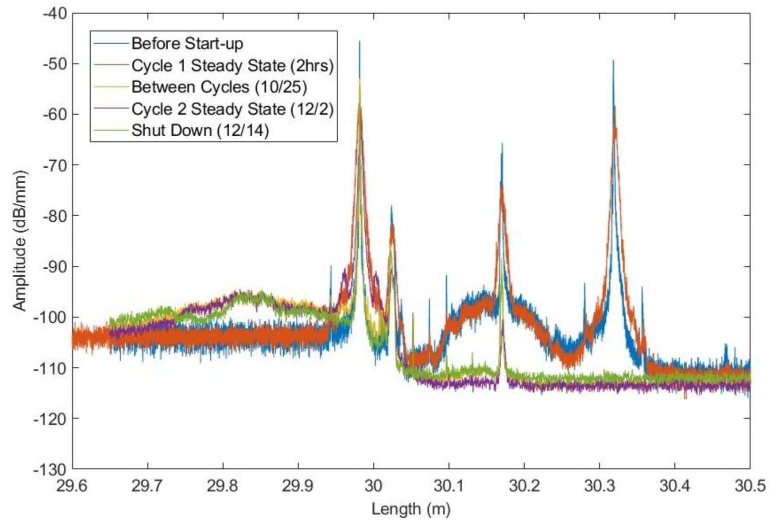

Figure 36. Sensor 3 before, during, and after irradiation.

The OFDR sensing at the location of the FBG for sensor 3 during startup is shown in Figure 37. The temperature fit used is a generic fit for sapphire optical fibers, and the individual sensor was not fully calibrated. The temperature reading is extremely noisy, possibly due to several different reasons. First, the features in all fibers become less defined after the fibers are installed in the reactor—a phenomenon potentially caused by significant physical vibration. Also, the backscatter profile of the sensor changes due to radiation damage. The signal is noisier than was expected based on previous irradiation results from OSURR. This fiber is a 100-um fiber, meaning it remains multi-modal, which can also contribute to the noise in an OFDR signal. The signal proved too noisy for iterative referencing to be successively employed to improve it; however, the fiber was re-referenced at about 3 hours into the irradiation, and that extended the signal response out to the initial 35 hours of irradiation (see Figure 38).

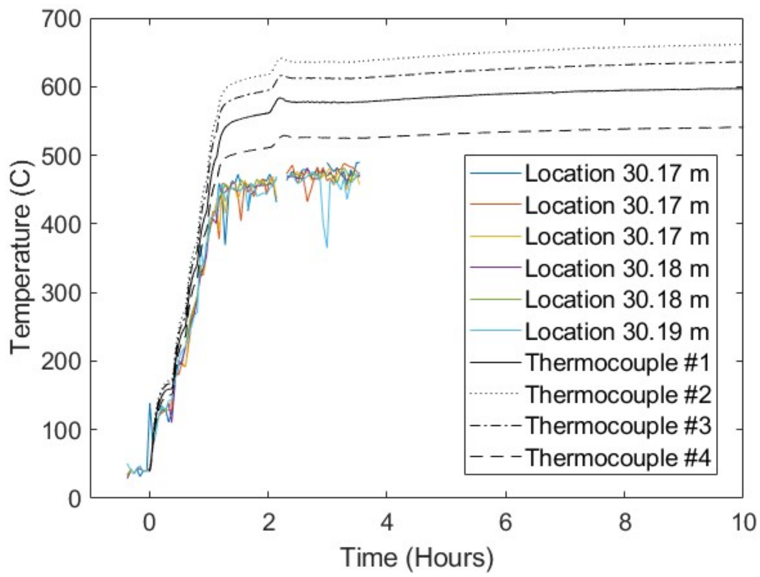

Figure 37. Sensor 3 temperature response to cycle 1 reactor startup, with no re-referencing.

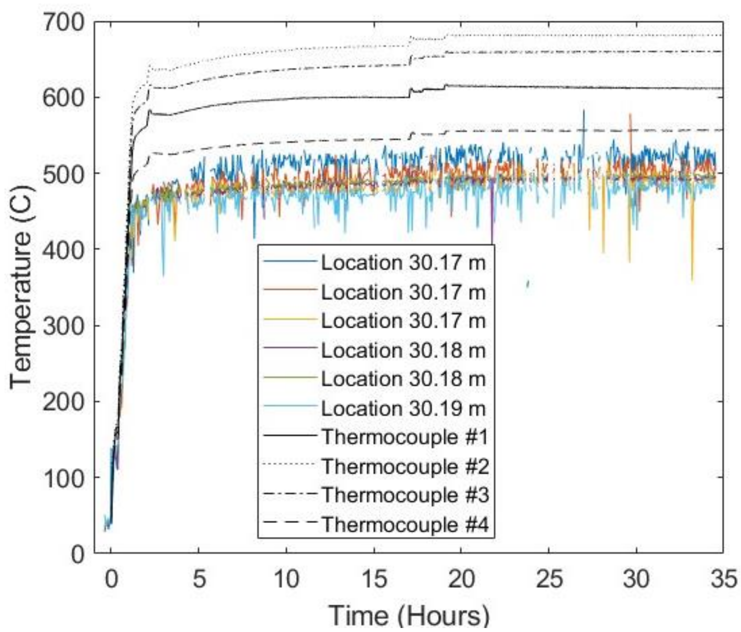

Figure 38. Sensor 3 temperature response to cycle 1 reactor startup, with re-referencing at 3 hours.

Sensors 4 and 5 are both 125-um-diameter sapphire optical fibers. Sensor 4 has four distinct FBGs, all positioned within the fuel region of the core. The top of the fuel is at 30.12 m along the length of the sensor. Figure 39 shows the backscatter profile of sensor 4 during the reactor startup, revealing a reduction in amplitude that does not level out. The gratings further down the fiber and further into the reactor core have a larger reduction in amplitude than those upstream. Figure 40 shows the sensor backscatter throughout the first 35 hours of irradiation. After 20 hours of irradiation, the bottom two gratings are completely attenuated. Figure 41 shows the backscatter profile before, during, and after both cycles of the irradiation. The FBGs in the sensor are completely attenuated by the end of the first irradiation cycle.

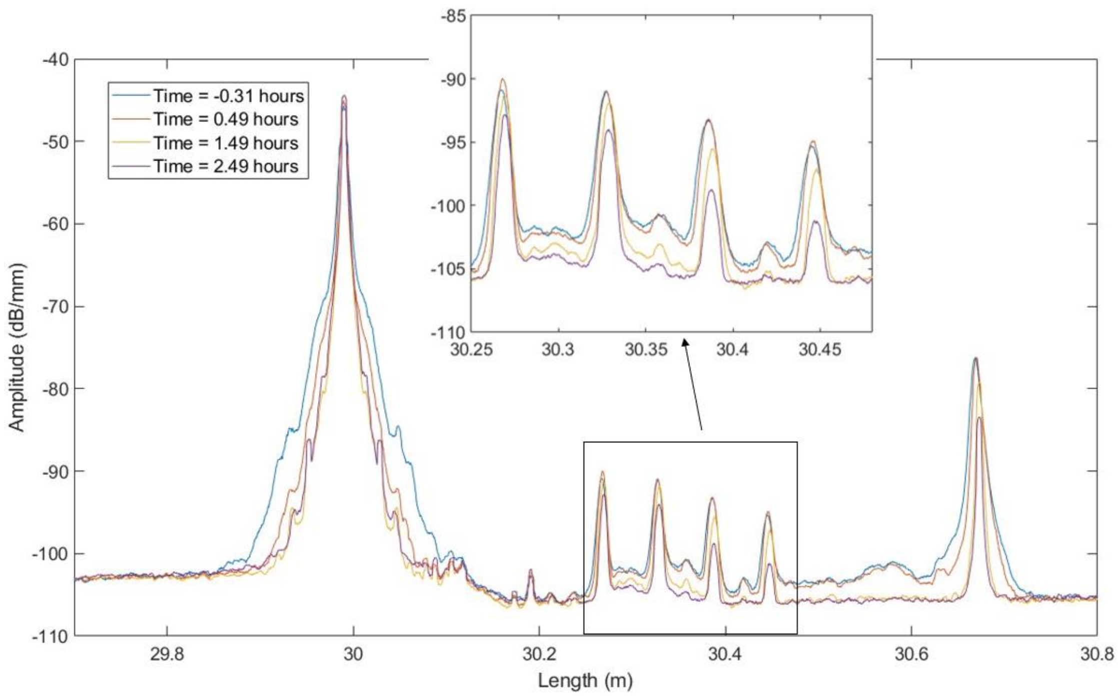

Figure 39. Sensor 4 during reactor initial startup for cycle 1.

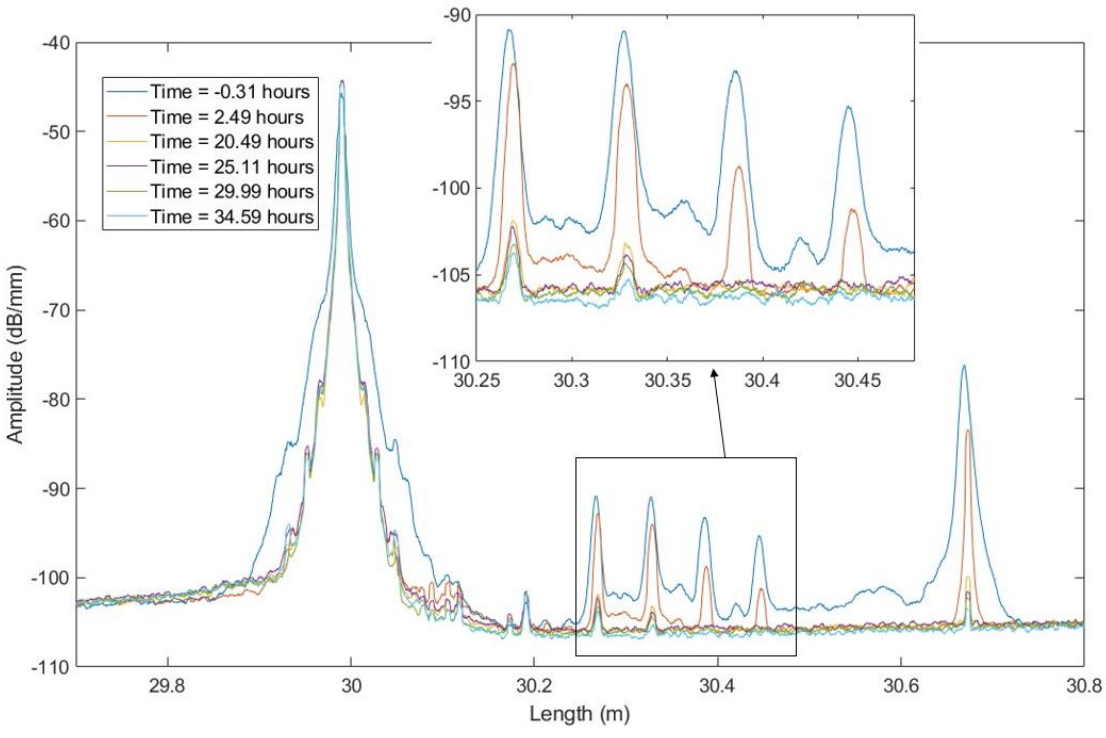

Figure 40. Sensor 4 during the initial reactor steady state for cycle 1.

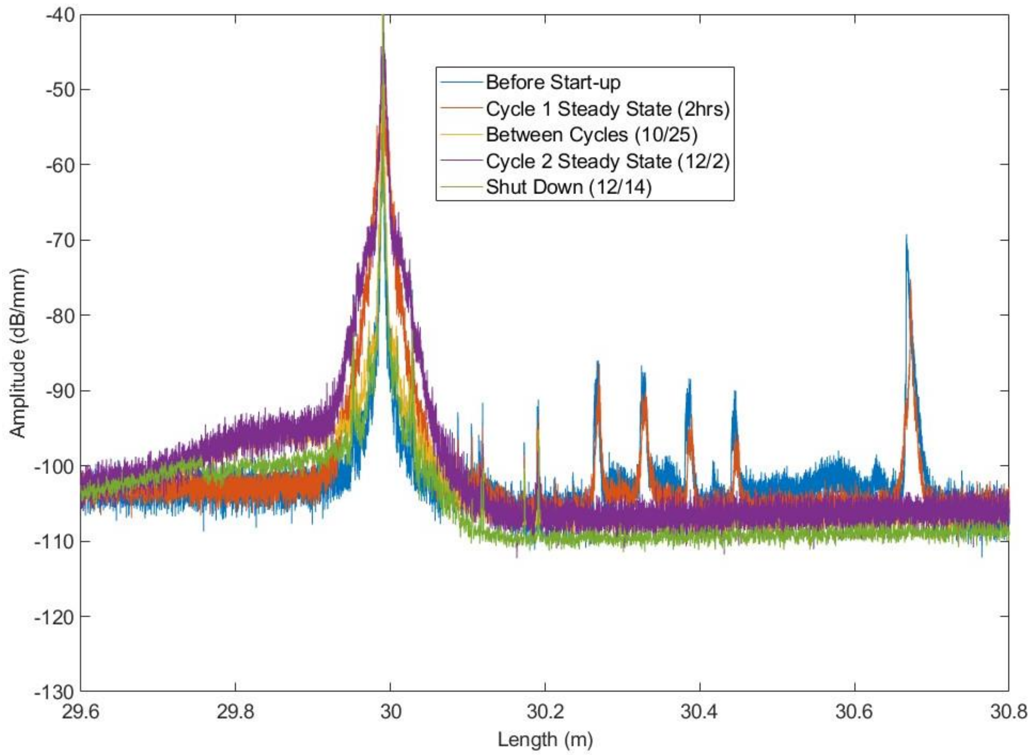

Figure 41. Sensor 4 before, during, and after irradiation.

Figure 42 shows the temperature response of sensor 4 at the FBG locations. The top two FBGs, while noisy, did last the first 35 hours of irradiation without re-referencing. The noise here is unsurprising, as the 125-um-diameter of the fiber makes it more multi-modal than a 100- or 75-um fiber.

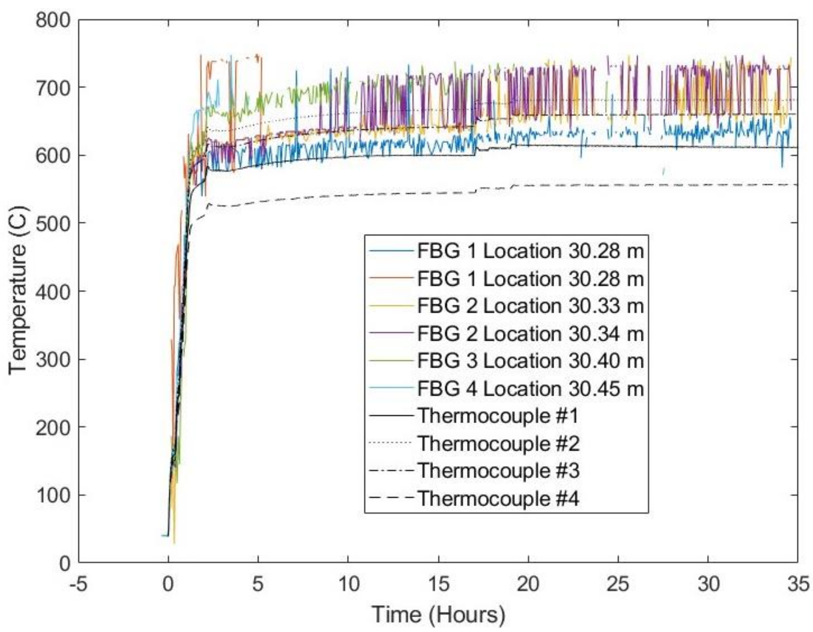

Figure 42. Sensor 4 temperature response to cycle 1 reactor startup, with no re-referencing.

Sensor 5 was also a 125-um-diameter sapphire fiber. Figure 43 and Figure 44 show the backscatter profile of the sensor throughout the startup and during the first 35 hours of irradiation. The top of the fuel is at 30.09 m with respect to the sensor length. There is an initial reduction in amplitude, just as with the other sensors. The OFDR signal from sensor 5 was too noisy to produce any meaningful temperature measurements.

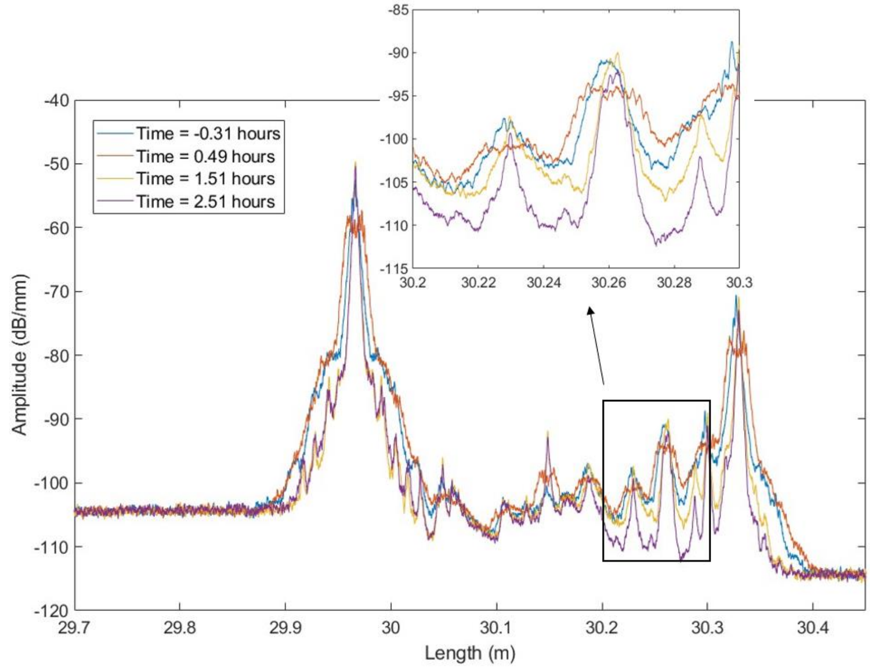

Figure 43. Sensor 5 during the initial reactor startup for cycle 1.

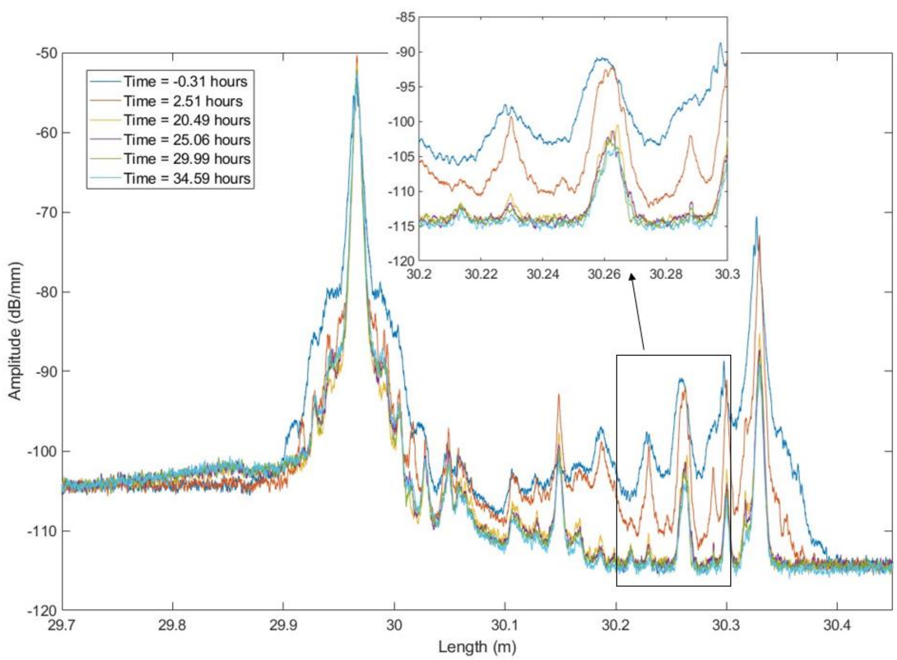

Figure 44. Sensor 5 during the initial reactor steady state for cycle 1.

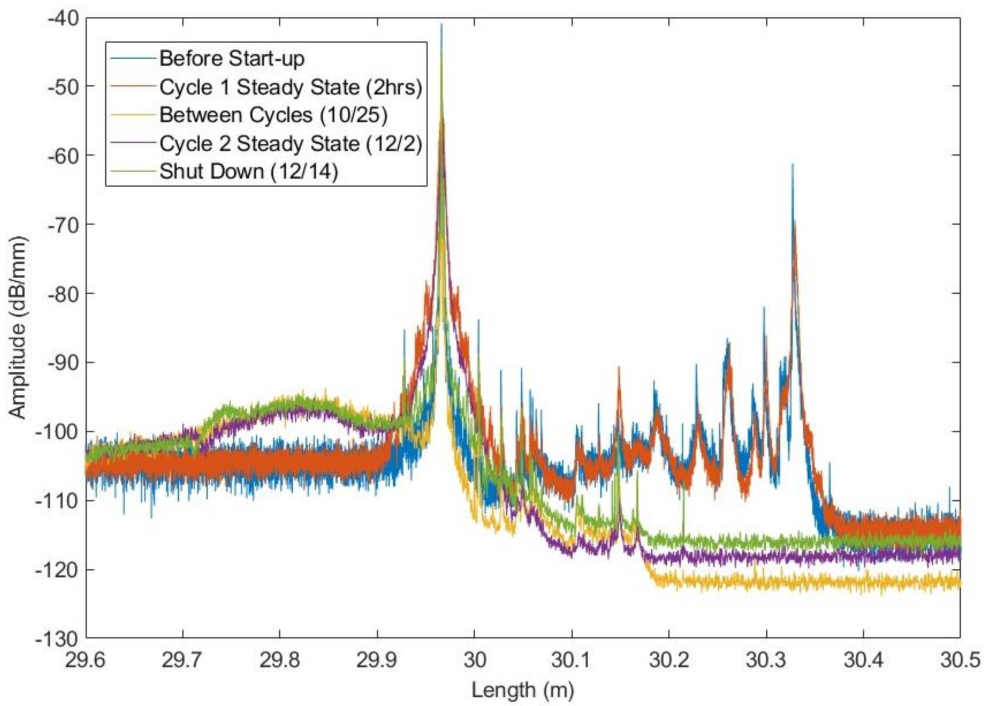

Figure 45. Sensor 5 before, during, and after irradiation.

Figure 45 shows the backscatter profile of sensor 5 before, during, and after both cycles of irradiation. The portion of the sensor inside the capsule is fully attenuated by the end of cycle 1. There is a noticeable difference between the attenuation of the fiber section that was heated and the section outside the graphite capsule. Recent work by Petrie et al. showed that attenuation in sapphire fiber due to radiation is temperature dependent and significantly increases at 688°C and above. [9] This work was conducted using sapphire wafers. Though the results here are insufficiently conclusive without conducting post-irradiation examination to determine the exact cause of the attenuation, it is likely due to radiation damage. Previous thermal-only work proved sapphire optical fibers to be stable at up to 1900°C. [10]

6. CONCLUSIONS AND RECOMMENDATIONS FOR FUTURE WORK

All the project objectives are complete. Interesting amplitude effects were observed at high temperatures in the sapphire fibers, both during in- and out-of-core testing. Further testing with clad optical fibers is required to determine the cause of the reversible amplitude reduction in sapphire fibers. The results of the present work indicate that distributed OFDR sensing in sapphire optical fiber is possible under certain conditions; namely, the sapphire fibers must be appropriately pretreated and have well-written defects inscribed so as to create a sable Rayleigh backscatter signal. This work indicates that sapphire optical fiber sensors are potentially suitable for ultra-high-temperature applications in which traditional silica optical fibers are prone to failure, such as long times above 700°C. Sapphire sensors represent a potential tool for use in experiments featuring temperatures exceeding 700°C for long periods to time, or for any time spent above 1000°C. Experiments featuring a low total fluence, such as irradiations in the Transient Reactor Test (TREAT) facility, also represent good applications for these sensors. Additional work is required to characterize the performance of the sapphire fiber cladding (which falls outside the scope of this project), as well as the effect of high temperature on the response of the fiber. A comprehensive material study is recommended as future work to evaluate attenuation in sapphire under irradiation, and how that attenuation changes with irradiation temperature. The drift and attenuation in the fiber at temperatures of up to 1600°C and total fluences of up to 2.9 $x10^{17}$ n/cm^2 were minimal, and the fibers returned to baseline after being heated to 1600°C under irradiation. This shows promise for future use of sapphire optical fibers in advanced reactors.

M2NA-19IN0107022: Year 1 Status Report; Complete 9/30/2020

M3NA-19IN0106014: Completion of sapphire fiber cladding process; Complete 03/19/2021

M3NA-19IN0106015: Experiment ready for insertion into heated OSURR irradiation: Complete 03/26/2021

M3NA-19IN0107028: Completion of out-of-pile testing; Complete 04/01/2021

M2NA-19IN0107026: Year 2 Status Report; Complete 9/29/2021

M3NA-19IN0107027: MITR experiment ready for insertion; Complete 7/8/2022

M3NA-19IN01070212: Completion of analysis of experimental results; Complete 3/30/2023

M3NA-19IN01070211: Submission of journal article; In-Progress

M2NA-19IN01070210: Final Report for (Project 19-16380) High-Fluence Active Irradiation and Combined Effects Testing of Sapphire Optical Fiber Distributed Temperature Sensors; Complete 10/09/2023

7. REFERENCES

1. McCary, K. M. and Daw, J. E. 2020. "Year 1 Status Report for Sapphire Irradiation Experiments." PRS/EXT-20-00672. http://www.micromaterialsinc.com/.

2. Wilson, B. A. and Blue, T. E. 2017. "Creation of an Internal Cladding in Sapphire Optical Fiber Using the ^{6}Li(n, alpha)^{3}H Reaction." *IEEE Sensors Journal*, **17**, no. 22, 7433-7439. https://doi.org/10.1109/JSEN.2017.2756448.

3. Spratt, W., et al. 2013. "Optical mode confinement and selection in single-crystal sapphire fibers by formation of nanometer scale cavities with hydrogen ion implantation." *Journal of Applied Physics*, **114**, 203501. https://doi.org/10.1063/1.4833240.

4. Jones, J.T., et al. 2021."Light Propagation Considerations For Internally Clad Sapphire Optical Fiber Using the 6Li(n,α)3H Reaction." *IEEE Journal of Lightwave Technology*, JLT-28482-2021. https://doi.org/10.1109/jlt.2021.3127863.

5. FemtoFiber Tec. Accessed September 2021. https://www.femtofibertec.de/en/home.

6. Wilson, B.A., Petrie, C.M., and Blue, T. E. 2018. "High-temperature effects on the light transmission through sapphire optical fiber." *J Am Ceram Soc*. **101**, no. 8, 3452–3459. https://doi.org/10.1111/jace.15515.

7. OSU Nuclear Reactor Lab. 2021. "Reactor Capabilities." The Ohio State University Nuclear Reactor Laboratory. https://reactor.osu.edu/research-capabilities/reactor-capabilities.

8. Petrie, C. M., Birri, A., and Blue, T. E. 2022. "Optical transmission and dimensional stability of single-crystal sapphire after high-dose neutron irradiation at various temperatures up to 688 °C." *Journal of Nuclear Materials*, **559**, no. 153432, ISSN 0022-3115, https://doi.org/10.1016/j.jnucmat.2021.153432.

9. Habisreuther, T., et al. 2015. "Sapphire fiber Bragg gratings for high temperature and dynamic temperature diagnostics." *Applied Thermal Engineering*, **91**, 860-865, ISSN 1359-4311, https://doi.org/10.1016/j.applthermaleng.2015.08.096.

10. Tobias Habisreuther, Tino Elsmann, Zhiwen Pan, Albrecht Graf, Reinhardt Willsch, Markus A. Schmidt, "Sapphire fiber Bragg gratings for high temperature and dynamic temperature diagnostics," *Applied Thermal Engineering*, Volume 91, 2015, Pages 860-865, ISSN 1359-4311, https://doi.org/10.1016/j.applthermaleng.2015.08.096.

Page intentionally left blank

Appendix A
MITR Irradiation Reports

MIT NUCLEAR REACTOR LABORATORY
AN MIT INTERDEPARTMENTAL CENTER

NSUF Subcontract 260687 – SFX Cycle 1 Irradiation Report

Prepared by David Carpenter
Irradiation Engineering
November 3, 2022

1. Summary

Per BEA subcontract 260687, the MIT NRL has designed, constructed, and operated an in-core irradiation vehicle as part of the NSUF project "High Fluence Active Irradiation and Combined Effects Testing of Sapphire Optical Fiber Distributed Temperature Sensors" led by Joshua Daw at the Idaho National Laboratory. The irradiation campaign at the MITR has been named the SFX, and consists of two MITR cycles of irradiation. In this experiment, optical fiber sensors will be interrogated in real-time during irradiation in inert gas at elevated temperatures to observe changes in their performance. The first cycle of irradiation (22Q3) has been completed and is described in this report.

2. Facility

The irradiations (and irradiation vehicle for this project), are named the SFX. The irradiations are being conducted in the core of the MIT Research Reactor (MITR), a 6 MW_{th} light water-cooled, heavy water and graphite-moderated research reactor operated by the MIT Nuclear Reactor Laboratory (NRL). The MITR operates continuously during quarterly cycles with several week outages in between for reactor and experiment maintenance activities.

The SFX experiment vehicle uses an inert gas irradiation facility located in the central ring of the MITR core. This facility provides controlled-temperature and instrumentation support for experiments up to 900°C. Thermal control is established primarily by the design of the facility, with active adjustment available by changing the cover gas mixture between helium and neon. As shown in Figure 1, the facility is placed in dummy fuel element within the MITR core, then extend upwards above the waterline in the primary gas plenum space (approximately 3m). This project utilized the FS-type vehicle design, shown for example in Figure 2, where the capsules are loaded into a shorter vehicle with a smaller diameter dry tube used only for cover gas and sensor/instrumentation lead-outs. However, the overall structure of these vehicles is similar and provides the same conditions to the test article.

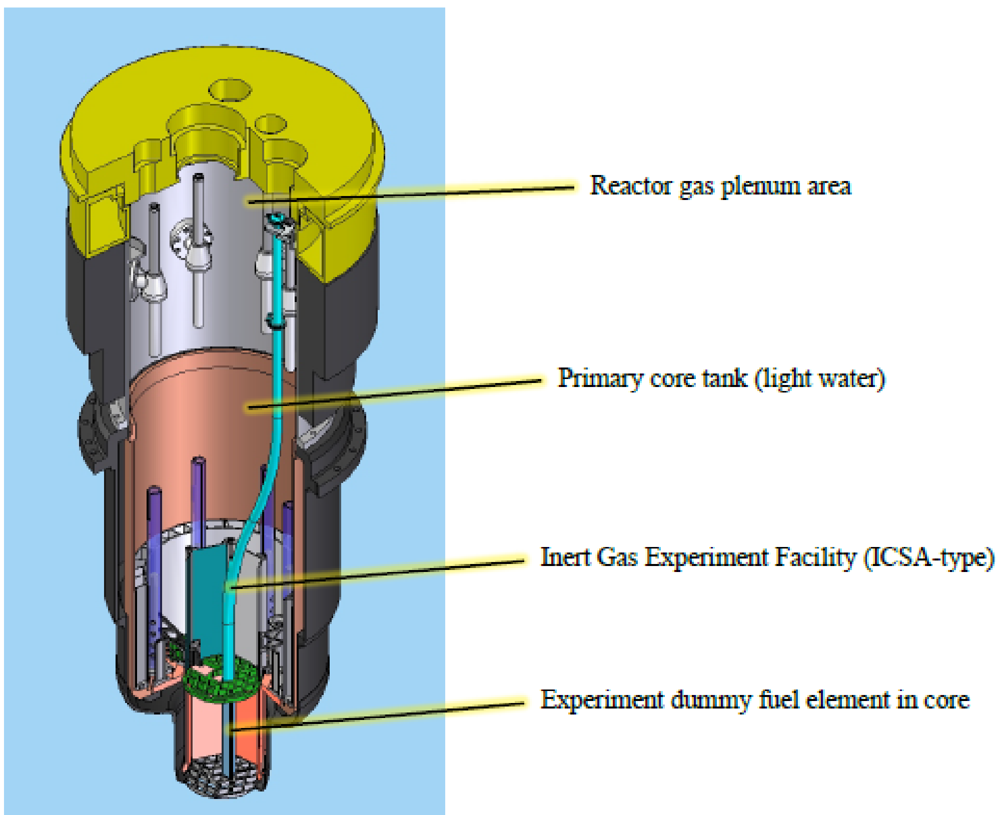

Figure 1. Positioning of a typical in-core inert gas irradiation facilities in the MITR.

Figure 2. Typical inert gas irradiation facility (FS-type).

Of the 27 fuel element positions, the three dedicated experiment positions within the MTIR core are shown in Figure 3 (with solid aluminum dummy elements installed). This project is utilizing position A-1 for both cycles of irradiation.

Figure 3. In-core irradiation positions.

3. SFX Irradiation

3.1. Test Plan

The project involves the irradiation of silica and sapphire optical fibers in the MITR core at elevated temperatures in a dry environment. The fibers (Table 1) were provided to MIT by INL in their completed configuration, with optical connectors at one end and sealed into 1/16-inch outer diameter steel guide tubes.

Table 1. Fiber sample descriptions.

Fiber	Composition	Number of Samples	Geometry
Sapphire optical fibers (bare; w/silica lead fiber)	Al_2O_3	5	18" length (+/-6"), 100 um diameter
Silica lead fiber	Silica (SiO_2) fluorine doped (proprietary), polyimide coated	3	Silica: 125 um diameter (+/-2 um), coating: 145 um diameter (+/-5 um)

The fibers are to be irradiated for two MITR cycles in an in-core position with 3×10^{13} n/cm^2/s thermal and 1×10^{14} n/cm^2/s fast neutron fluxes in a dry, inert gas environment. Using nuclear heating and helium/neon cover gas temperatures are to be controlled to a nominal 600±50°C. Optionally, limited temperature ramping during irradiation can be conducted to temperatures up to 750°C. The cover gas flow will be regulated around 50 cc/min flow rate and 20 psig static pressure.

3.2. Experiment Vehicle Design

The SFX irradiation vehicle was designed to fit within the standard A-1 experiment dummy fuel element (Figure 4) and dry irradiation thimble (Figure 5). Inside the thimble is the sample fixturing, which for this experiment consists of a single capsule to support the fibers.

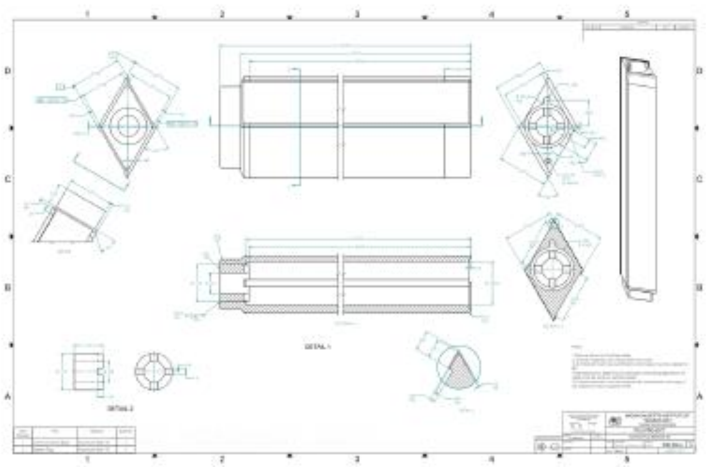

Figure 4. A-1 dummy fuel element.

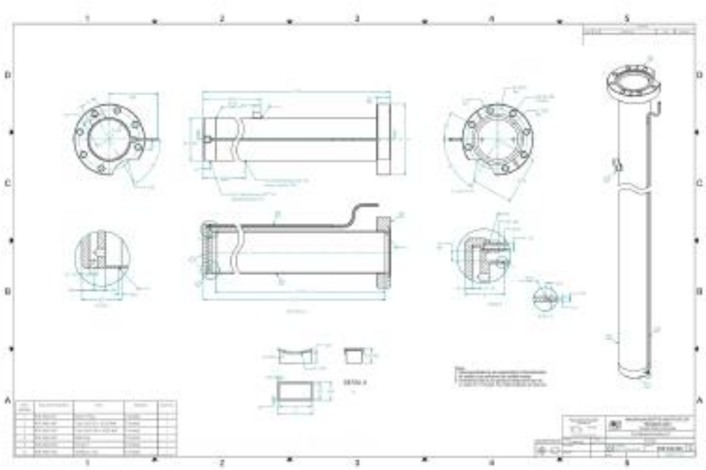

Figure 5. A-1 dry irradiation thimble.

The SFX capsule assembly (Figure 6) has an outer titanium capsule with inner graphite liner. The titanium and graphite parts were sized to both hold the in-core portions of the fiber guide tubes in position and also provide appropriate mass and thermal conduction volumes to generate the desired temperatures at the fibers. There is a central tungsten alloy spine that supports the capsule and a titanium clamp above the capsule, which secures the lead-outs to prevent shifting during vehicle assembly and installation.

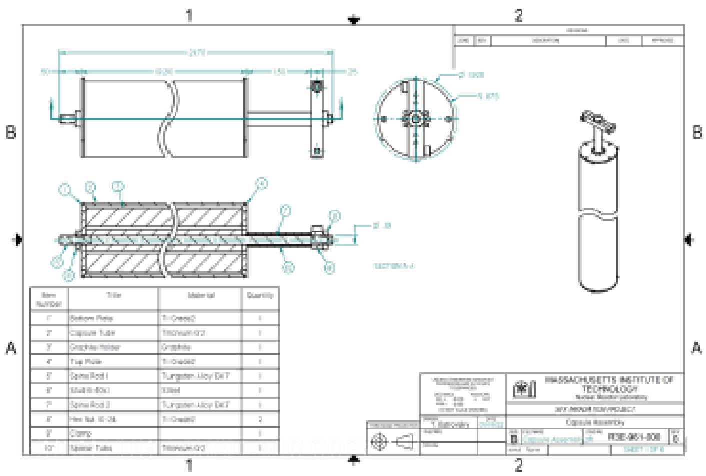

Figure 6. SFX capsule assembly.

The eight fiber guide tubes provided by INL were indexed FT1 through FT8 (see Table 2), and positioned around a single circular diameter in the graphite holder, interspersed with 1/16-inch type-K thermocouples for temperature measurement. These thermocouples, TC1-TC4, were placed at different axial positions to observe the axial temperature variations along the fibers. The locations of the fiber sensors and thermocouples are given in Figure 7 and Figure 8.

Table 2. SFX fiber sensor designations.

INL Designation	Sensor Description	MIT Designation
1	Al2O3-75-1	FT1
2	Al2O3-125-1	FT2
3	Al2O3-100-2	FT3
4	Al2O3-125-1	FT4
5	Al2O3-125-2	FT5
6	Dead End Silica	FT6
7	SiO2-FBG-1	FT7
8	SiO2-FBG-1	FT8

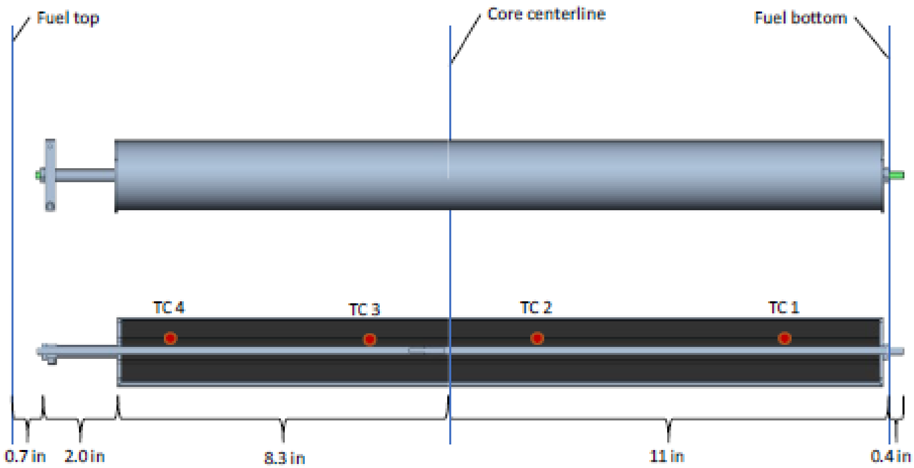

Figure 7. SFX in-core capsule assembly layout.

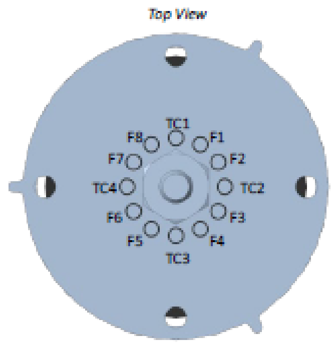

Placement
(bottom of sensor exterior housing relative to core centerline)

Sensor	Rel. Position (in)
TC1	-8.0
TC2	-2.0
TC3	+2.0
TC4	+7.0
F1-F8	-10.8

Figure 8. SFX sensor and sample placement.

3.3. Pre-Irradiation Examination

Prior to this SFX irradiation, samples of the fiber and guide tubes materials were provided to MIT for neutron activation analysis and were irradiated using the MITR pneumatic irradiation facility. The fiber sensors arrived pre-loaded into their respective steel guide tubes, and no additional pre-irradiation examination was conducted at MIT.

4. Irradiation History

The SFX vehicle was installed in the MITR core position A-1 on July 19th, 2022 for the 22Q3 operations cycle. Initial reactor startup to full power (5.7 MW) occurred on July 20th. Fiber interrogation and data collection was performed by INL-supplied electronics. This data was gathered separately from the NRL experiment data acquisition.

The experiment was initially set to hold at 635°C using its helium/neon cover gas mixture auto controller, but this was later increased to 675°C and was maintained there for the remainder of the cycle. The reactor shut down for the end of cycle on September 30th, 2022, and the experiment was temporarily removed from the core and relocated to the in-vessel storage ring during refueling operations on October 3rd, 2022.

The (MCNP-calculated) accumulated neutron (Figure 9) and gamma fluence based on the measured reactor operational history is given in Table 3. The temperature, power, and cover gas histories for this cycle are given in Figure 10 and Figure 11. During this cycle the SFX accumulated 368.1 MWd of irradiation at temperature.

During this cycle there were six periods of reduced power operation or reactor shutdown. Only one, on September 17th, 2022, was related to the SFX. On the 17th the cover gas mass flow controller management unit failed, causing a loss of all cover gas flow to the vehicle. This resulted in a cover gas pressure decrease within the vehicle and 20°C increase in the SFX peak graphite temperature over a 10-minute period before reactor power began to decrease. During the troubleshooting and management unit replacement the reactor power was lowered to 1 MW. Normal cover gas flow, full reactor power, and temperature was restored after four hours.

Table 3. Calculated average in-core flux and fluence for the SFX capsule for cycle 22Q3.

	Flux ($1/cm^2$-s)	Fluence ($1/cm^2$)	Exposure (MGy)
Total Neutron	2.4E+14	1.3E+21	-
Thermal Neutron (< 1 eV)	3.4E+13	1.9E+20	-
Fast Neutron (>0.1 MeV)	1.1E+14	6.4E+20	-
Fast Neutron (>1 MeV)	5.2E+13	2.9E+20	-
Gamma	2.6E+14	1.5E+21	1.5E+4

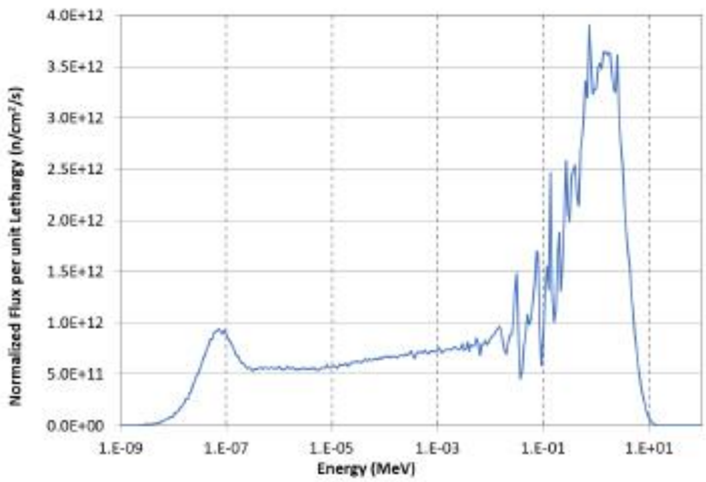

Figure 9. Neutron energy spectrum in the A-1 position for a dry experiment.

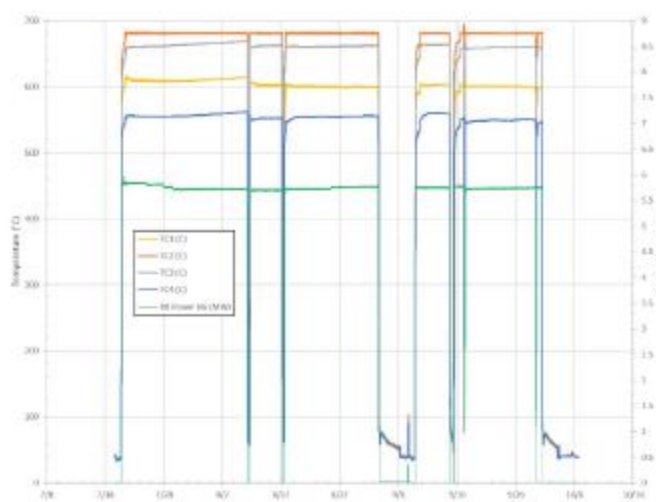

Figure 10. SFX cycle 1 temperature and power history.

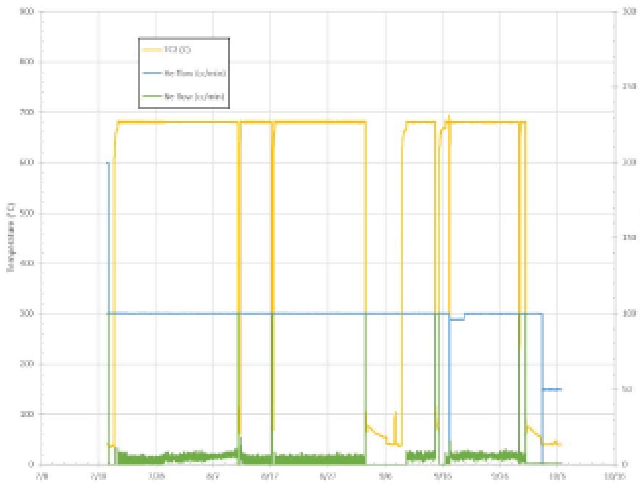

Figure 11. SFX cycle 1 cover gas composition history.

5. Post-Irradiation Activities

The SFX vehicle will be irradiated for a second cycle in the same configuration in the same in-core position. No inter-cycle examination or configuration changes are expected. It is planned to be re-installed and irradiated during MITR cycle 22Q4 completing on December 23rd, 2022.

NSUF Subcontract 260687 – SFX Cycle 2 Irradiation Report

Prepared by David Carpenter

Irradiation Engineering

March 27, 2023

1. Summary

Per BEA subcontract 260687, the MIT NRL has designed, constructed, and operated an in-core irradiation vehicle as part of the NSUF project "High Fluence Active Irradiation and Combined Effects Testing of Sapphire Optical Fiber Distributed Temperature Sensors" led by Joshua Daw at the Idaho National Laboratory. The irradiation campaign at the MITR has been named the SFX, and consists of two MITR cycles of irradiation. In this experiment, optical fiber sensors will be interrogated in real-time during irradiation in inert gas at elevated temperatures to observe changes in their performance. The second cycle of irradiation (22Q4) has been completed and is described in this report.

2. Facility

The irradiations (and irradiation vehicle for this project), are named the SFX. The irradiations are being conducted in the core of the MIT Research Reactor (MITR), a 6 MW_{th} light water-cooled, heavy water and graphite-moderated research reactor operated by the MIT Nuclear Reactor Laboratory (NRL). The MITR operates continuously during quarterly cycles with several week outages in between for reactor and experiment maintenance activities.

The SFX experiment vehicle uses an inert gas irradiation facility located in the central ring of the MITR core. This facility provides controlled-temperature and instrumentation support for experiments up to 900°C. Thermal control is established primarily by the design of the facility, with active adjustment available by changing the cover gas mixture between helium and neon. As shown in Figure 1, the facility is placed in dummy fuel element within the MITR core, then extend upwards above the waterline in the primary gas plenum space (approximately 3m). This project utilized the FS-type vehicle design, shown for example in Figure 2, where the capsules are loaded into a shorter vehicle with a smaller diameter dry tube used only for cover gas and sensor/instrumentation lead-outs. However, the overall structure of these vehicles is similar and provides the same conditions to the test article.

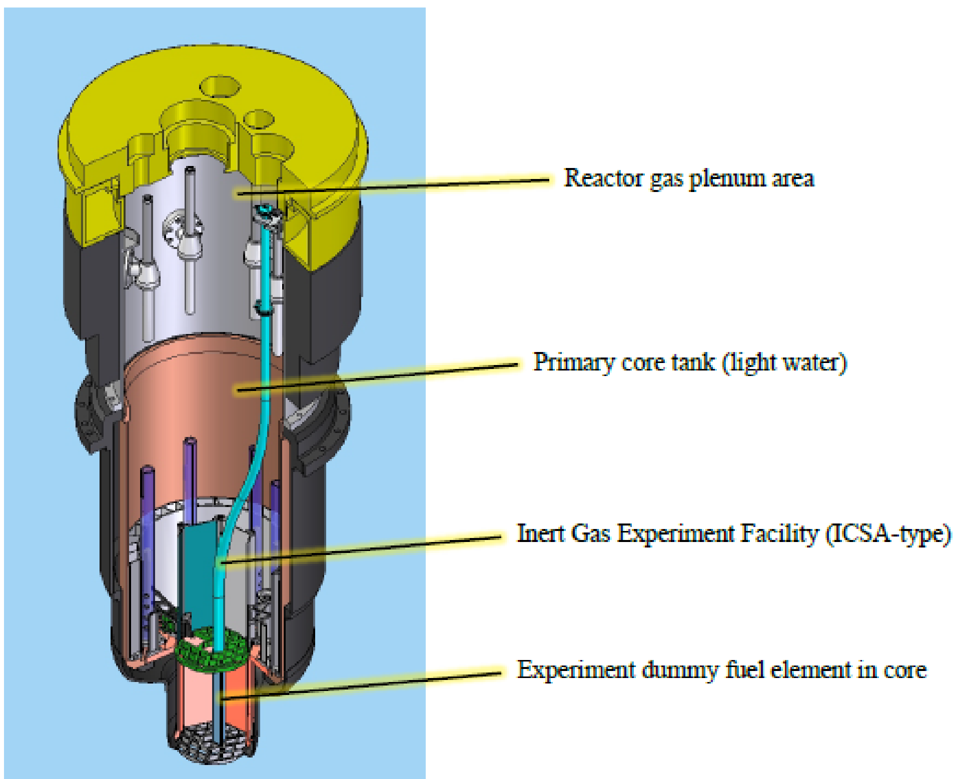

Figure 1. Positioning of a typical in-core inert gas irradiation facilities in the MITR.

Figure 2. Typical inert gas irradiation facility (FS-type).

Of the 27 fuel element positions, the three dedicated experiment positions within the MTIR core are shown in Figure 3 (with solid aluminum dummy elements installed). This project is utilizing position A-1 for both cycles of irradiation.

Figure 3. In-core irradiation positions.

3. SFX Irradiation

3.1. Test Plan

The project involves the irradiation of silica and sapphire optical fibers in the MITR core at elevated temperatures in a dry environment. The fibers (Table 1) were provided to MIT by INL in their completed configuration, with optical connectors at one end and sealed into 1/16-inch outer diameter steel guide tubes.

Table 1. Fiber sample descriptions.

Fiber	Composition	Number of Samples	Geometry
Sapphire optical fibers (bare; w/silica lead fiber)	Al_2O_3	5	18" length (+/-6"), 100 um dia.
Silica lead fiber	Silica (SiO_2) fluorine doped (proprietary), polyimide coated	3	Silica: 125 um dia. (+/-2 um), coating: 145 um dia. (+/-5 um)

The fibers were irradiated for two MITR cycles in an in-core position with $3x10^{13}$ n/cm^2/s thermal and $1x10^{14}$ n/cm^2/s fast neutron fluxes in a dry, inert gas environment. Using nuclear heating and helium/neon cover gas temperatures are to be controlled to a nominal 600±50°C. Optionally, limited temperature ramping during irradiation can be conducted to temperatures up to 750°C. The cover gas flow will be regulated around 50 cc/min flow rate and 20 psig static pressure.

3.2. Experiment Vehicle Design

The SFX irradiation vehicle was designed to fit within the standard A-1 experiment dummy fuel element (Figure 4) and dry irradiation thimble (Figure 5). Inside the thimble is the sample fixturing, which for this experiment consists of a single capsule to support the fibers.

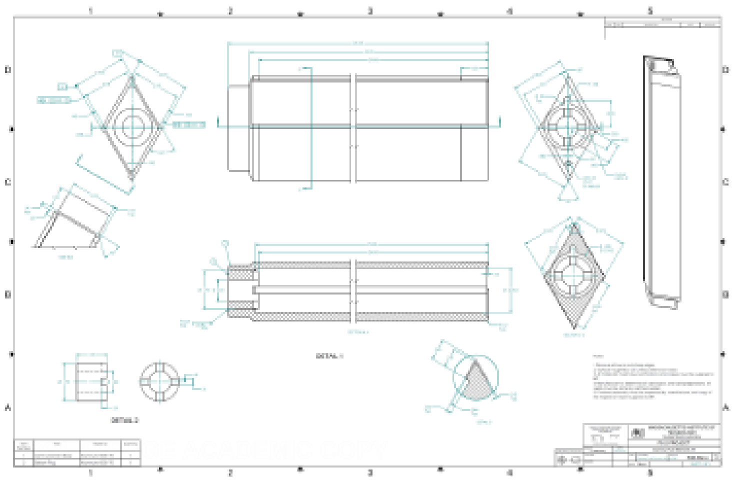

Figure 4. A-1 dummy fuel element.

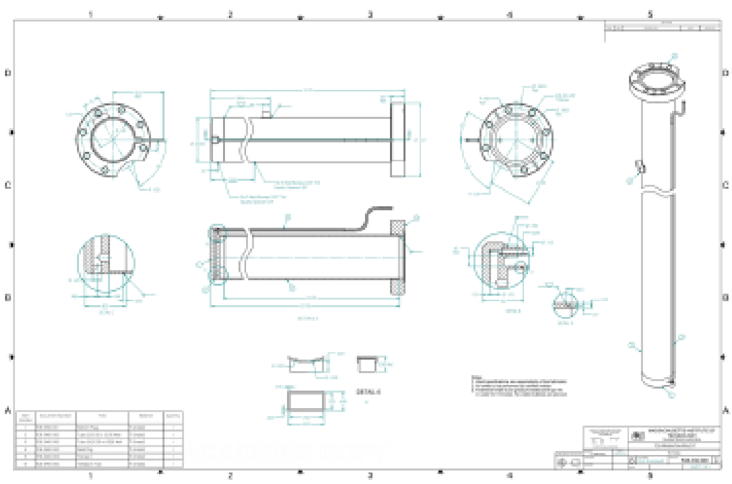

Figure 5. A-1 dry irradiation thimble.

The SFX capsule assembly (Figure 6) has an outer titanium capsule with inner graphite liner. The titanium and graphite parts were sized to both hold the in-core portions of the fiber guide tubes in position and also provide appropriate mass and thermal conduction volumes to generate the desired temperatures at the fibers. There is a central tungsten alloy spine that supports the capsule and a titanium clamp above the capsule, which secures the lead-outs to prevent shifting during vehicle assembly and installation.

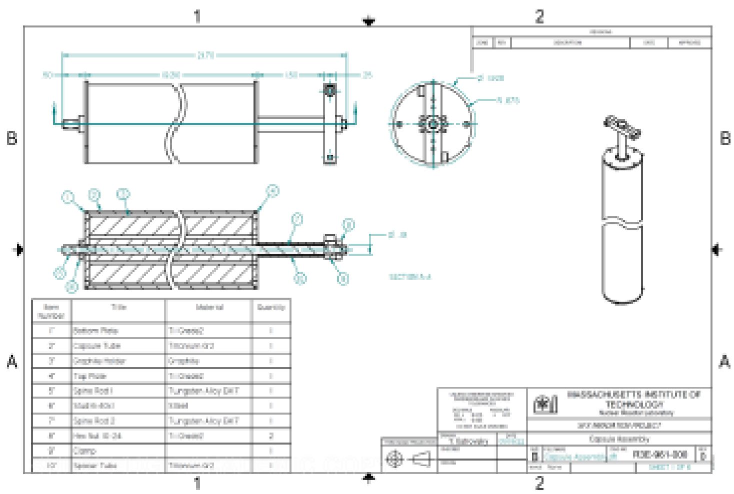

Figure 6. SFX capsule assembly.

The eight fiber guide tubes provided by INL were indexed FT1 through FT8 (see Table 2), and positioned around a single circular diameter in the graphite holder, interspersed with 1/16-inch type-K thermocouples for temperature measurement. These thermocouples, TC1-TC4, were placed at different axial positions to observe the axial temperature variations along the fibers. The locations of the fiber sensors and thermocouples are given in Figure 7 and Figure 8.

Table 2. SFX fiber sensor designations.

INL Designation	Sensor Description	MIT Designation
1	Al2O3-75-1	FT1
2	Al2O3-125-1	FT2
3	Al2O3-100-2	FT3
4	Al2O3-125-1	FT4
5	Al2O3-125-2	FT5
6	Dead End Silica	FT6
7	SiO2-FBG-1	FT7
8	SiO2-FBG-1	FT8

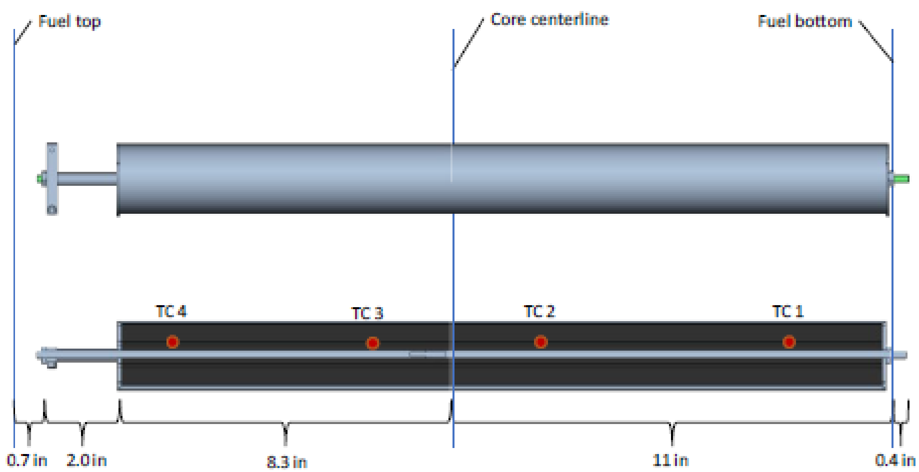

Figure 7. SFX in-core capsule assembly layout.

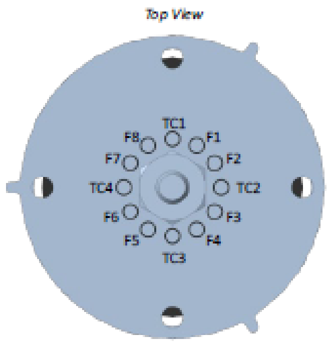

Placement
(bottom of sensor exterior housing relative to core centerline)

Sensor	Rel. Position (in)
TC1	-8.0
TC2	-2.0
TC3	+2.0
TC4	+7.0
F1-F8	-10.8

Figure 8. SFX sensor and sample placement.

4. Irradiation History

The SFX vehicle was first installed in the MITR core position A-1 on July 19th, 2022 for the 22Q3 operations cycle and was discharged on October 3rd, 2022 during the planned reactor outage. This previous irradiation history is covered in detail in the Cycle 1 Irradiation Report. The SFX vehicle was returned to the A-1 position on October 7th (Figure 9), however due to reactor maintenance activities the reactor startup to full power (5.7 MW) did not occur until November 29th. As before, fiber interrogation and data collection on the fiber response was performed by INL-supplied electronics, while experiment temperature and gas and reactor parameters were gathered separately by the NRL experiment data acquisition system.

Figure 9. SFX vehicle re-installed in the MITR core on December 7th, 2022.

After reaching full reactor power, the experiment was programmed to return to the previous cycle's temperature setpoint of 680°C on thermocouple #2 (TC2) and hold. Except for a short period of reactor low-power operation on December 7th due to an un-related issue, the SFX maintained this temperature until the end of the cycle. The reactor was shut down for the end of cycle earlier than expected on December 12th, 2022 due to a reactor maintenance issue. The experiment was transferred from the reactor core to the main NRL hot cells on December 19th to prepare for disassembly and post-irradiation examination.

The (MCNP-calculated) accumulated neutron (Figure 10) and gamma fluence based on the measured reactor operational history is given in Table 3; the total accumulated values are given in Table 4. The temperature, power, and cover gas histories for this cycle are given in Figure 11 and Figure 12. During this cycle the SFX accumulated 73.4 MWd of irradiation at temperature, for a total of 441.5 MWd over both cycles.

Table 3. Calculated average in-core flux and fluence for the SFX capsule for MITR cycle 22Q4.

	Flux (1/cm^2-s)	Fluence (1/cm^2)	Exposure (MGy)
Total Neutron	2.4E+14	2.6E+20	-
Thermal Neutron (< 1 eV)	3.4E+13	3.8E+19	-
Fast Neutron (>0.1 MeV)	1.1E+14	1.3E+20	-
Fast Neutron (>1 MeV)	5.2E+13	5.8E+19	-
Gamma	2.6E+14	2.6E+20	3.1E+03

Table 4. Total accumulated average fluence for the SFX capsule.

	Fluence (1/cm^2)	Exposure (MGy)
Total Neutron	1.6E+21	-
Thermal Neutron (< 1 eV)	2.3E+20	-
Fast Neutron (>0.1 MeV)	7.6E+20	-
Fast Neutron (>1 MeV)	3.5E+20	-
Gamma	1.6E+21	1.9E+04

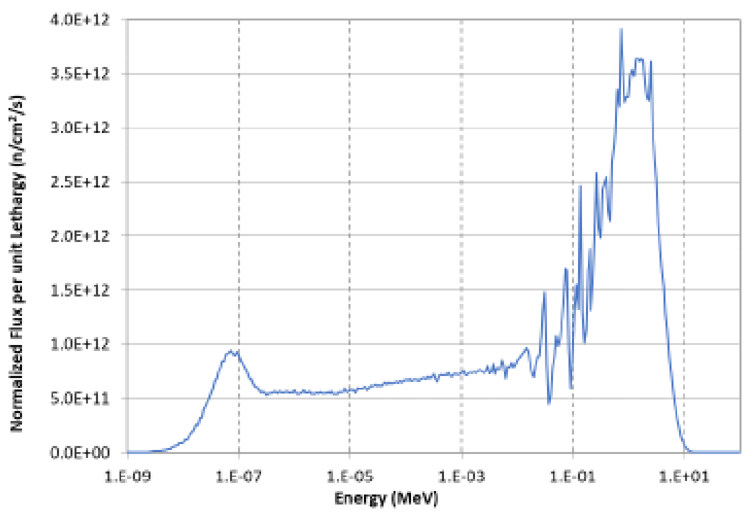

Figure 10. Neutron energy spectrum in the A-1 position for a dry experiment.

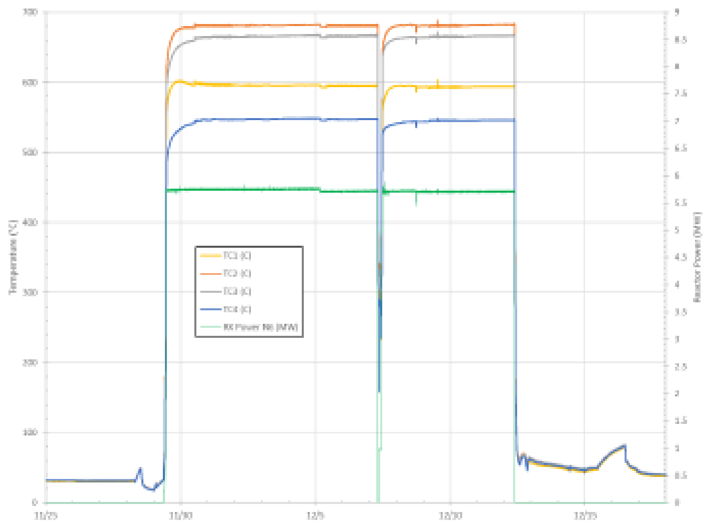

Figure 11. SFX Cycle 2 temperature and power history.

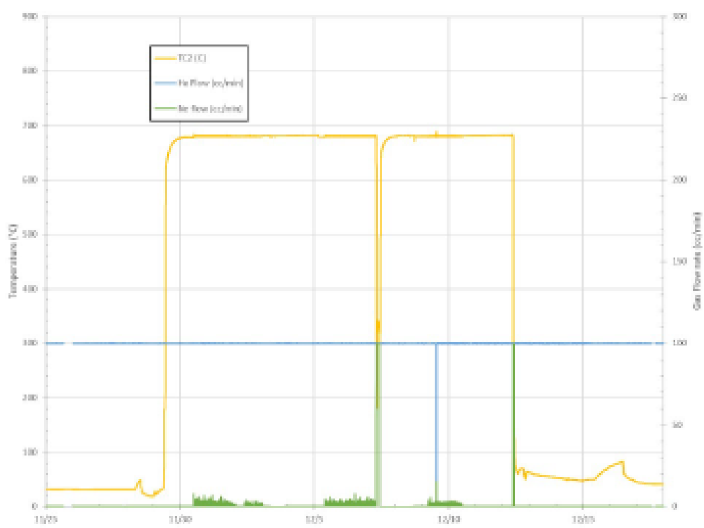

Figure 12. SFX Cycle 2 cover gas composition history.

5. Post-Irradiation Activities

With the conclusion of the second cycle, no additional irradiation is planned for the SFX vehicle. Due to the short 22Q4 cycle, additional resources are available to conduct some post-irradiation disassembly and examination on the vehicle. The initial effort is focused on extraction of the fibers by removing them from the steel guide tubes. Previous experience with this type of configuration has shown that it is sometimes possible to extract whole fiber lengths from the tubes after cutting away the guide tube at the far end of the fiber where radiation levels are low. Given the composition, it is expected that the fiber itself will have low activity, dominated by small amounts of surface contamination from the guide tube.

If the fibers are able to move freely within the guide tubes they will each be extracted and undergo gentle surface decontamination followed by visual inspection and documentation. Gamma spectra and absolute activities will be obtained for each fiber and they will be repackaged for storage until additional examinations are possible. Progress on the extraction and PIE of the fibers will be detailed in a later report.